KINETIC STUDIES OF NANOSECOND, MICROSECOND, AND MILLISECOND COMPONENTS OF DELAYED LIGHT EMISSION FROM THE ALGAE SCENEDESMUS OBLIQUUS WITH A NEWLY DEVELOPED PHOTON COUNTING APPARATUS

Thesis for the Degree of Ph. D.

MICHIGAN STATE UNIVERSITY

HARRY CLARK BEALL

1972

This is to certify that the

thesis entitled
KINETIC STUDIES OF NANOSECOND, MICROSECOND, AND MILLISECOND COMPONENTS OF DELAYED LIGHT EMISSION FROM THE ALGAE SCENEDESMUS OBLIQUUS WITH A NEWLY DEVELOPED PHOTON COUNTING APPARATUS

presented by

HARRY CLARK BEALL

has been accepted towards fulfillment
of the requirements for

Ph. D. degree in Biophysics

A. Haug
Major professor

Date 2 Nov. 1972

ABSTRACT

KINETIC STUDIES OF NANOSECOND, MICROSECOND, AND MILLISECOND COMPONENTS OF DELAYED LIGHT EMISSION FROM THE ALGAE SCENEDESMUS OBLIQUUS WITH A NEWLY DEVELOPED PHOTON COUNTING APPARATUS

By

Harry Clark Beall

Delayed light emission was measured from the wild-type D_3 strain, from the mutant 8 strain, and from the mutant 11 strain of Scenedesmus obliquus algae. The algae were illuminated by 488 nm laser light which was modulated on and off by either a rotating slotted disc or by an electro-optical laser light modulator. The instantaneous intensity of the stimulus laser light at the algal sample was in the range of 12 to 30 milliwatts per square centimeter for all experiments. The kinetics of the light emission from the algae were measured through a 690 nm optical interference filter during the time intervals between the stimulus laser light flashes. The delayed light emission was measured over the first five millisecond time period following the extinction of the stimulus light.

The D_3 wildtype strain and mutant 8 produced delayed

light emission of an intensity which could be measured, while any emission present from mutant 11 was not intense enough to be recorded by the electronic apparatus. This indicated that most, if not all, of the delayed light emission originated from photosystem II.

The delayed light emission curve for the wildtype and mutant 8 strains decayed in a complex fashion, i.e., the delayed light emission decay curves could not be described analytically by a single exponential term.

The initial microsecond section of the delayed light emission curve intersected the prompt fluorescence decay curve at virtually a right angle for both the wildtype and the mutant 8 algae. The lack of a transition zone between the two curves indicated that the prompt fluorescence was not a fast component of delayed light emission. Instead, the lack of a transition zone between the two curves is evidence that delayed light emission occurred concurrently with prompt fluorescence during the periods the algae were exposed to the laser light. Following the instant the stimulus laser light was extinguished, the prompt fluorescence intensity fell to zero and the presence of the less intense delayed light emission was revealed.

The intensity of light emission from an algal sample was measured: (a) a few microseconds before the stimulus light was extinguished, and (b) in the first microsecond

after the stimulus light was extinguished. Since the delayed light emission decay curve was found to be rather flat throughout the first microsecond following stimulus light extinction, the ratio of prompt fluorescence intensity to delayed light emission intensity could be closely approximated as the ratio of (a)/(b). This ratio was found to be of the order of 170:1 for the wildtype algae and 170:0.25 for the mutant 8 algae. These ratios were obtained from algae after 20-minute periods of preillumination by the modulated laser light.

When dark-adapted algae were used in the above ratio experiments, the results were different. The wildtype algae maintained a ratio comparable to the ratio measured after illumination. However, the mutant 8 algae were found to emit more delayed light during the first seconds of illumination. The dark-adapted mutant 8 algae gave a ratio of 80:1.

The final set of experiments in this thesis measured the changes in intensity of the first 60 microseconds of delayed light emission from the wildtype and mutant 8 algae as the dark-adapted algae went through light induction periods of 820 seconds. The results showed that the intensity of the first 60 microseconds of delayed light decreased during the first 30 to 40 seconds of the induction period in the case of the wildtype algae, but then recovered to a

level comparable to the first few seconds. The mutant 8 algae, however, showed different kinetics in that the intensity of the delayed light decreased from the first few seconds of illumination, and no recovery in intensity was seen. These experimental results were interpreted as evidence in support of the hypothesis that delayed light emission was proportional in intensity to the rate of electron flow through photosystem II.

In order to accomplish the above measurements of delayed light emission, a photon counting system was constructed. This electronic instrumentation was operated in three different modes: pulse-height analysis, recurrent multiscaling, and single sweep multiscaling. All three modes were illustrated by the various experiments of the thesis.

The photon counting apparatus was used especially to study the entire nanosecond and microsecond ranges of delayed light emission, ranges which have never been accessible to detailed study.

KINETIC STUDIES OF NANOSECOND, MICROSECOND, AND MILLISECOND COMPONENTS OF DELAYED LIGHT EMISSION FROM THE ALGAE SCENEDESMUS OBLIQUUS WITH A NEWLY DEVELOPED PHOTON COUNTING APPARATUS

By

Harry Clark Beall

A THESIS

Submitted to
Michigan State University
in partial fulfillment of the requirements
for the degree of

DOCTOR OF PHILOSOPHY

Department of Biophysics

1972

To Ping

ACKNOWLEDGMENTS

I wish to express my sincere appreciation to my major professor, Dr. A. Haug for his most enthusiastic support and guidance during the course of these investigations. The constructive criticism and advice of the thesis committee members, Dr. A. El-Bayoumi, Dr. D. Lamport, and H. T. Tien are also greatly appreciated. I would like to express my thanks to Dr. A. Lang for enabling me to carry out these investigations in the MSU/AEC Plant Research Laboratory.

I wish to thank Dr. N. I. Bishop of Oregon University for suppling the mutant 8 and mutant 11 strains of Scenedesmus algae, and Mr. D. Jaquet for his assistance with the maintenance of the algal culture. Special thanks go to Mr. Bob Geyer for the design and construction of the mechanical apparatus used in this work.

This work was supported by United States Atomic Energy Commission Contract #AT-(11-1)-1338. The personal financial assistance from United States Public Health Service Training Grant #GM-01422 from the United States National Institutes of Health is also acknowledged and appreciated.

TABLE OF CONTENTS

LIST OF TABLES

LIST OF FIGURES

Figure Page

Figure Page

LIST OF PUBLICATIONS FROM THE THESIS

1. A. Haug, D. D. Jaquet and H. C. Beall. Time-resolved spectroscopy of light emitted from Scenedesmus obliquus measured under steady-state conditions between five nanoseconds and several seconds. Biophys. J., 4, 33a (1971).

2. A. Haug, D. D. Jaquet and H. C. Beall. Delayed light emission from the algae Scenedesmus obliquus, measured under steady-state conditions from four nanoseconds to ten seconds. Biophys. J., 12, 86a (1972).

3. H. C. Beall and A. Haug. A photon counting system for measurement of algal delayed light emission. Biophys. J., 12, 144a (1972).

4. A. Haug, D. D. Jaquet and H. C. Beall. Light emission from the Scenedesmus obliquus wildtype, mutant 8 and mutant 11 strains, measured under steady-state conditions between four nanoseconds and ten seconds. Biochim. Biophys. Acta, 283, 92 (1972).

5. H. C. Beall and A. Haug. A photon counting device for the measurement of nanosecond and microsecond kinetics of light emission from biological systems. Anal. Biochem., in press.

INTRODUCTION

Approximately 100 years ago, fluorescence was observed in illuminated green plants (1). Delayed light emission was discovered in green plants in 1951 (2). The delayed light emission has the same spectrum as that of the "prompt" fluorescence which algae emit while being illuminated (3, 4). Thus, it has been proposed that the delayed light emission originates from the same singlet state from which the prompt fluorescence originates (3). The majority of both delayed light emission and fluorescence seems to originate in photosystem II (5). Most photosynthetic organisms exhibit both prompt fluorescence and delayed light (6). All green algae, blue-green algae, brown algae, and land plants give about the same intensity of delayed light emission when tested under equivalent conditions (7). It has been concluded that the striking similarity of delayed light decay curves, for all plants that oxidize water to oxygen, implies that the early steps in quantum conversion must be the same for all these plants (8).

Delayed light emission has been studied as a photochemical mechanism for thirty years. Certain types of organic molecules can emit both prompt fluorescence and a delayed light emission following excitation by an intense flash of light. The prompt fluorescence is the short-lived fluorescence that occurs as the molecule reverts from the first excited singlet state to the ground state. Most fluorescent organic molecules have prompt fluorescence lifetimes of 10^{-8} to 10^{-9} seconds.

Delayed light emission, delayed fluorescence, has the same emission spectrum as prompt fluorescence in organic molecules, but the lifetime of the delayed fluorescence is orders of magnitude longer than the corresponding prompt fluorescence.

There have been two physical mechanisms described in the photochemical literature to explain the majority of the observations of delayed emission in organic molecules. The first of these was called "alpha-phosphorescence" by Lewis, Lipkin, and Magel (9) who postulated that the molecule could be excited to the first excited singlet and thence to the lowest triplet state via intersystem crossing. From the metastable triplet state, the molecule could be thermally excited to the singlet state and emit delayed fluorescence as the molecule reverted to the ground state. Since a thermal excitation was necessary to move the electron from the triplet state to the singlet, the energy

spacing between these two levels had to be rather small for this type of delayed fluorescence to occur. Also, the observed radiative lifetimes of the delayed fluorescence and phosphorescence were identical when this mechanism was responsible for delayed fluorescence. The alpha-phosphorescence type of delayed light emission has also been labelled as "E-type delayed fluorescence" (10).

A second type of delayed fluorescence, P-type delayed fluorescence, can occur in rigid glass at 77 ^{o}K as in liquid solutions of certain organic molecules. This process exhibits biphotonic kinetics, i.e., two photons of excitation light must be absorbed for each delayed fluorescence photon emitted by the sample. P-type delayed emission has been postulated to occur as a result of triplet-triplet annihilation in which two triplet states interact to produce one excited singlet state and one ground singlet state. The excited singlet state could then produce prompt fluorescence when it reverted to the ground state (11).

Various mechanisms have been proposed to explain the origin of delayed light from green plants and algae (2, 12, 13). Arnold and Azzi suggested that there are three to four separate mechanisms producing the delayed light which is observed from photosynthetic tissues (12). They postulated that the delayed light in the time range of 1 to 100 milliseconds after stimulus light extinction was due to a

recombination of electrons and holes. This is a biphotonic process. For the longer time ranges of delayed light, they postulated that thermal excitation could lift an electron from the level of ferredoxin (in the Z scheme) to the level of chlorophyll. This process is a single photon process. As a third process, they suggested that some of the longer duration delayed light was due to the process of untrapping of holes from semiconductor-type material in the photosynthetic apparatus. A fourth process involved oxygen in the light emission process.

Arnold and Sherwood (14) and Arnold (15) supported the hypothesis of a solid-state mechanism for delayed light emission because of experiments in which the thermoluminescence (glow curves) recorded from frozen dried chloroplast films exactly mimiced the results obtained with semiconductor materials.

Sweetser (6) pointed out that delayed light emission was sensitive to light intensity, temperature, and chemical inhibitors of photosynthesis. This early study of delayed light emission warned that delayed light could not exhibit simple decay kinetics because this light component depended upon other chemical species for the gain or loss of energy. Thus, they postulated that the halflife of the delayed light emission would reflect the concentrations of enzymes and cofactors involved in the decay process. They did not favor the theory of recombination of trapped electrons and

holes as the mechanism responsible for delayed light emission. Instead, the concluded that all evidence pointed to delayed light emission being caused by a reversal of electron flow at a point early in the oxygen-liberating pathway.

In the paper first describing delayed light emission from plant material, Strehler and Arnold (2) concluded that the delayed light process was an indication of the reversibility of some early reactions in photosynthesis, including at least one enzymatic reaction. The conclusion was based on the observations that delayed light emission and photosynthesis followed the same temperature dependence, UV light destroyed the delayed light emission at the same rate as that of photosynthesis, delayed light emission and photosynthesis saturated at the same intensity of light, and chemicals which inhibited photosynthesis were found to inhibit delayed light emission. They concluded that the delayed light emission decay could be interpreted as a series of reactions which fed back to the excited state.

Strehler (16) continued to maintain that the delayed light emission was a chemiluminescence and not a physical phosphorescence because of a demonstration that delayed light emission and photosynthesis saturated at the same light intensity, while the physical process should not have shown a saturation. Goedheer (17), however, later concluded that the light saturation of photosynthesis occurred at

much higher intensity than that of delayed light emission.

Another line of evidence that perhaps the delayed light emission process could depend upon an enzymatic series of reactions originates in the reports of light emission from chloroplasts which had been stimulated by acid-base transitions (18, 19) and by KCl and NaCl concentration gradients (20). The acid-base luminescence had the same spectrum as delayed light emission and the luminescence was prevented from occurring by the photosynthetic poison 3-(3,4-dichlorophenyl)-1,1-dimethylurea, DCMU. DCMU did not prevent ATP generation by the acid-base transition, however.

G. W. Robinson has tried to describe the attractive features of the primary photosynthetic steps being based upon energy transfer and energy multiplication via the triplet state of chloroplyll (21-23). He specifically mentioned the possibility of triplet exciton migration through pigment aggregates and he outlined the process of triplet exciton fusion in which two triplet excitons could mutually annihilate one another to produce one molecule in the ground state with the other molecule promoted to a higher electronic state having perhaps up to twice the energy of the triplet state.

Stacy et al. have utilized the triplet exciton fusion mechanism to fashion a model for the kinetics of the delayed light emission from Chlorella (24). They observed that the

delayed light intensity was proportional to the square of the exciting light intensity, a fit which was predicted by the model. The model also predicted that the delayed light intensity could be affected by a magnetic field, but no magnetic field effect was observed. Also, they observed no *in vivo* phosphorescence which would have given direct confirmation of the presence of triplet states *in vivo*.

In order to cite the triplet exciton fusion process as the mechanism for delayed light emission, the delayed light emission intensity should be proportional to the square of the excitation light intensity. Jones (25) has shown that, in completely dark-adapted plants, the intensity of delayed light after a single flash of low intensity light was proportional to the excitation flash intensity. However, Ruby (26, 27) has found that the delayed light emission is proportional to both the intensity of a single flash and to changes in the yield which is established by previous flashes. He concluded that the intensity dependence may appear to be close to the square of intensity of excitation light, even though it is in fact linear for a single flash.

Both the triplet-triplet fusion model and the electron-hole recombination model fail to account for the fact that delayed light emission can not be observed from photosynthetic tissue held at a temperature below zero degrees Centigrade. In fact, in the original paper (2) describing

delayed light emission in plants, the authors pointed out that delayed light emission intensity seemed to show the same dependence upon temperature as did the overall photosynthetic rate. In this first paper was the conclusion that the delayed light emission was due to a reversibility of some early reactions in photosynthesis, including at least one enzymatic reaction.

In summary, several theories have been formulated to explain the delayed light emission of photosynthesis on a physical basis. In order to be universally accepted, however, a theory of the mechanism of delayed light emission must be compatible with the general theory, or model, of photosynthesis. The most popular model of photosynthesis at the present time is the so-called "Z-scheme" which was first described by Hill and Bendall (28).

According to the Z-scheme, there are two photosystems which act in series to accomplish the process of photosynthesis. The two photoreactions are coupled by a complex electron transfer chain which can move electrons from photosystem II, the oxygen-evolving photosystem, to photosystem I, the CO_2-reducing photosystem. In the electron transfer chain connecting the two photosystems, there is located at least one site of phosphorylation.

The illumination of photosynthetic cells with light absorbed mainly by photosystem I results in the oxidization

of the components of the electron transport chain between the two photosystems, while illumination with light absorbed by photosystem II results in the reduction of the components of the electron transport chain. Long periods of darkness can also result in the oxidation of the electron transport chain (29) and the hypothetical photosystem II reaction centers, consisting of the "fluorescence quencher" pigment Q. Thus, after a period of darkness, the photosystem II reaction centers are almost all in the "open trap" form, Q. Upon illumination, the reaction centers change to the "closed trap" form, Q^-. The photosystem II traps can also be closed by chemical reducing agents and opened by oxidizing agents. When dark-adapted algae are first illuminated, the traps are in the open form and there is observed a certain fluorescence yield. After initiation of illumination, the traps eventually close and the fluorescence yield increases. Thus, the fluorescence yield can be monitored as an indicator of the condition of the reaction center traps of photosystem II.

Equilibria studies with the electron transport chain between the two photosystems and studies of the fluorescence yield and of oxygen evolution (30, 31, 32) have given evidence for an electron acceptor compound, called A, which transfers electrons from the photosystem II trap, Q^-, to the first element of the electron transport chain. This

transfer step (33) is the site of action of the photosynthesis inhibitor compound DCMU. The electron acceptor compound A is present in a 12 to 20 fold higher concentration (32) than Q; thus, there is said to exist a "pool" of the compound A at a site in the electron transport chain next to Q.

Characterization of Scenedesmus Algae

N. I. Bishop (34) has isolated and characterized several mutants of the green algae Scenedesmus obliquus for use in photosynthesis research (35). The mutant strains numbered eight and eleven have been particularily useful and these mutants have been well characterized (36, 37). Bertsch et al. have summarized the characteristics of these two strains (5). Table 1 lists this summary of the two mutant strains as compared to the wildtype strain. The essence of the Table 1 information is that mutant 8 algae have a functional photosystem II and a defective photosystem I, while mutant 11 algae have a functional photosystem I and a defective photosystem II. Careful examination of the mutant 8 and mutant 11 algae revealed (34) that the major pigments, such as the chlorophylls, carotenes, and carotenoids were present in proper concentration.

During illumination, wildtype Scenedesmus algae can be expected to maintain a rather constant flow of electrons through the electron transport chain joining the two

Table 1. Listing of the characteristics of Scenedesmus wildtype algae, mutant 8 algae, and mutant 11 algae (5).

	Wildtype	Mutant 8	Mutant 11
Autotrophic growth	+	0	0
Heterotropic growth (dark + glucose)	+	+	+
Pigmentation	Normal	Normal	Normal
Respiration	Normal	Normal	Normal
Presence of hydrogenase	+	+	+
Photoreduction of CO_2 with H_2	+	0	+
Quinone Hill reaction	+	+	0
Presence of P700	+	0	+
Presence of narrow, rapid EPR signal	+	0	+
Presence of broad, slow EPR signal	+	0	+
All glow curve peaks present	+	+	0
Photosystem I active	+	0	+
Photosystem II active	+	+	0

photosystems because photosystem II (the source of the electrons) can function and because photosystem I (the drain for the electrons) can function also. On the other hand, mutant 8 Scenedesmus algae can not be expected to maintain as high an electron flow through the electron transport chain as the wildtype algae. The reason is that the lack of the photosystem I trap pigment, P700, in the mutant 8 algae results in a block in the major route of exit for the electrons injected into the electron transport chain by photosystem II.

Thesis Hypothesis

The hypothesis of this thesis work is that photosynthetic delayed light emission intensity reflects the rate of electron flow through photosystem II. Furthermore, the site of origin of delayed light emission must be at, or on the photosystem II side of, the transfer point of electrons from the primary electron acceptor, A, to the electron transport chain between the two photosystems.

One of the implications of the above hypothesis is that the so-called delayed light emission also occurs during periods of illumination of photosynthetic tissue, but that the delayed light emission can not be observed until the stimulus light is extinguished. That this statement is reasonable will be shown in the first section of this thesis in which the first nanoseconds and first microseconds of the

delayed light emission curve were recorded by the photon counting technique of pulse-height analysis. The delayed light emission decay curves recorded in the first section of results chapter always had a negative slope, and the origin of the delayed light emission curve showed no transition region at the instant of the stimulus light extinction. Instead, the abrupt decay of the prompt fluorescence, at the instant of stimulus light extinction, intersected the initial observable portion of the delayed light emission curve at a right angle, implying that the delayed light emission occurred during illumination and was observed only when the prompt fluorescence ceased.

If, as the hypothesis of this thesis states, the delayed light emission intensity depends upon the rate of electron flow through photosystem II, one would also expect a constant ratio between the intensity of photosystem II fluorescence and the intensity of delayed light emission, when both are measured under steady-state conditions of illumination. That is to say, once the wildtype algae had acclimated to a modulated stimulus light of a given intensity, a certain rate of electron flow between the two photosystems would be expected. This flow rate should remain rather constant as long as the stimulus illumination continued at constant intensity. The prompt fluorescence would also be expected to reach a constant level of intensity

during a period of illumination with a given level of stimulus light intensity. Therefore, it would be expected that the ratio of the prompt fluorescence intensity to the intensity of the first microsecond of delayed light would be a certain constant value. The mutant 8 algae, however, would be expected to maintain a lower intensity of delayed light emission than the wildtype after acclimation to the stimulus light because of the lower rate of electron flow between the two photosystems due to the defective photosystem I of the mutant 8 algae. The second part of this thesis describes the measurement of the prompt fluorescence to delayed light ratio from single samples of wildtype and mutant 8 algae by the pulse height analysis technique of photon counting. The ratio was measured under the experimental conditions in which the algae had been acclimated to the stimulus light for a period of thirty minutes, and the ratio was also measured under conditions in which dark-adapted algae were first exposed to the modulated stimulus light. The results of these experiments confirmed the above hypothesis. The following three paragraphs outline previous work that has been done for the purpose of establishing the exact relationship between the prompt fluorescence and the delayed fluorescence.

Arnold and Davidson (38) have suggested that a large percentage of the emission from Chlorella that is usually labelled as prompt fluorescence may in fact be the delayed

light emission. This conclusion was prompted by the following observations. They made a double logarithmic plot of the algal light emission intensity as a function of time after stimulus light extinction. A decay curve describing data from in vivo fluorescence lifetime experiments was plotted from the 10^{-9} second region of the plot toward the 10^{-8} second time region. Delayed light emission data were plotted from the 10^{-1} second region to the 10^{-4} second region. The latter data formed a smooth curve which rose in amplitude as the curve extended toward the shorter time regions. Between 6.5×10^{-4} seconds to 4×10^{-3} seconds, the delayed light emission signal was found to be approximately proportional to 1/t. An extrapolation of the delayed emission curve to an intersection with the 10^{-8} second lifetime region of the fluorescence decay curve showed that a large percentage of the fluorescence curve would lie beneath the intersection point. Thus, the conclusion was made that the majority of the emission that had been called fluorescence was actually due to delayed light emission.

Müller and Lumry (39) were the first to attempt to measure the relative intensities of the total fluorescence emission and that of delayed light. Their experiments utilized phase-fluorometric measurements. They found that 90 percent of the total emission was prompt fluorescence and 10 percent was delayed light.

Very recently, Arnold (40) has utilized an electric

field effect to stimulate a ten-fold increase in delayed light emission some 30 seconds following a flash of low intensity incandescent light in broken Chrnopodium chloroplasts. Assuming that a ten-fold increase would also be observed in the delayed light emission component of the total emission during illumination, and assuming that the electric field did not influence the level of prompt fluorescence, Arnold calculated that the ratio of delayed light emission to fluorescence intensity equaled 70/10,000.

When photosynthetic organisms that have been adapted to darkness are illuminated, the observable parameters of the photosynthetic process undergo a peculiar sequence of changes called the induction effect. Joliot (41, 30) has studied extensively the kinetics of oxygen evolution by means of brief flashes of light on dark-adapted algal samples. The induction effect on prompt fluorescence has been studied in somewhat more detail than delayed light induction (42). The last sections of the thesis contain experiments which examine the changes in delayed light emission intensity during the induction period for both the wildtype algae and the mutant 8 algae. These two algal strains should exhibit different kinetics of delayed light emission during the induction period for the following reasons. As mentioned previously, the photosystem II traps become oxidized during periods of darkness, and the compounds of

the electron transport chain also become oxidized. Upon illumination, the wildtype algae would be expected to maintain a rather constant flow of electrons through photosystem II during the induction period because both the photosystems in the wildtype algae are functional. Therefore, the delayed light emission intensity should remain rather constant during the induction period for the wildtype algae. On the other hand, the mutant δ algae perhaps could maintain an electron flow through photosystem II comparable to that of the wildtype algae for only a few seconds until the oxidized pool of the electron acceptor compound A began to be depleated. The electron flow rate would then decline. If the hypothesis that delayed light emission reflects the electron flow rate is correct, the decline in the rate of electron flow should be reflected in a corresponding decline in the intensity of delayed light emission. The third section of the thesis describes experiments utilizing the recurrent multiscaling photon counting technique to record the change in intensity of the first five milliseconds of the delayed light emission decay curve for the wildtype algae and the mutant δ algae during induction periods of δ20 seconds. The fourth section of the thesis describes an experimental procedure in which an electronic gating system was used in conjunction with single sweep multiscaling photon counting in order to count only those photons of delayed light

emission which occurred within a 60-microsecond interval following the instant of each light extinction of the modulated stimulus light.

INSTRUMENTATION

This instrumentation chapter is divided into seven sections. The first section presents a general description of the theory of single photon detection and counting. The second section presents a description of the specific single photon detection system used in all of the experiments of the thesis. The third section of this chapter presents a description of the two methods of stimulus light modulation used in the experiments of this thesis. The fourth section of this chapter presents a description of the technique of pulse-height analysis, as used in certain experiments of this thesis. The fifth section of this chapter describes the instrumentation which was used to record the waveform of the stimulus light modulation by the electro-optical laser modulators. The sixth section of this chapter presents a description of the recurrent multiscaling technique, as used in certain experiments of this thesis. The seventh section of this thesis chapter presents a description of the single sweep multiscaling technique, a technique of photon counting used in the last experiments reported in this thesis.

Photon Counting

During the last ten years, the technique of photon counting has spread from its origin in the field of astronomy to other areas of science. The field of Raman spectrometry has especially benefitted from application of the technique (43). However, there have been several papers describing utilization of photon counting techniques in biological research. Two recent papers (44, 45) reported very successful application of the technique in experiments designed to measure changes in fluorescence polarization from fluorescent probe molecules attached to macromolecules.

The photon counting method is the method of choice when attempting to measure low light levels with an acceptable signal-to-noise ratio (43). The theory (46, 47) and application fundamentals (48, 54) of the photon counting technique have been discussed in the last few years, as have the criteria for evaluating and selecting photomultiplier tubes for photon counting (55, 56). Other papers have been concerned with critical evaluation of the photon counting technique as compared to synchronous detection (57, 58) and to lock-in amplifiers, and noise voltage methods (59, 60).

The essential component of a photon counting system is a photomultiplier tube which is operated with an anode load

impedance of such low value that the output RC time constant of the detection system is in the range of one to two nanoseconds. With such a low time constant, there is virtually no RC integration at the anode output of the tube. Light quanta striking the photocathode of the photomultiplier tube eject single electrons from the cathode surface. Because of the secondary emission process in the dynode chain of the photomultiplier tube, a single primary electron ejected from the photocathode surface can result in a charge of 10^6 electrons arriving at the anode simultaneously. This burst of electric charge produces a voltage pulse of millivolt amplitude across the anode load resistor. These voltage pulses are amplified, and fed to a discriminator which rejects all pulses of amplitude lower than a certain preset trigger level. For each pulse that does trigger the discriminator input circuit, the discriminator output circuit produces a single standardized output pulse of much larger voltage amplitude and duration. All of the discriminator output pulses are identical, and they may be counted by high-speed counters, or they may be processed by other digital instrumentation.

Photon counting has several advantages over the conventional analog technique of measuring low levels of light intensity. First, when photon counting instrumentation is properly designed and operated, single light quanta events

can be detected. This represents the ultimate in detection of low level light intensities. Furthermore, the properly designed system also exhibits a wide dynamic range, and thus the system can be used as a radiometer over three to five orders of magnitude of light intensity up to the point of photomultiplier tube overload.

Another advantage of photon counting is that the discriminator rejects most of the low amplitude noise pulses which contribute to the "dark current" in the conventional analog light detection system.

A fourth advantage of photon counting is the time resolution that the system can achieve. The more modern photomultiplier tubes have transit times of one to two nanoseconds, and the amplifiers commercially available at the present time have wide bandwidths. Discriminators have response times in the order of a few nanoseconds. Thus, a photon counting system can measure a low-level light signal which abruptly changes intensity over a time interval of two or three nanoseconds.

Since single photon detection is basically a digital technique, the discriminator pulses can easily be processed by digital counters, or, as will be described later, the discriminator pulses can be processed by a time-to-amplitude converter and an analog-to-digital converter and the information accumulated in a multichannel analyzer.

After completion of a photon counting experiment, the accumulated data form a high resolution histogram in the memory array of the multichannel analyzer. A Polaroid photograph can record the data curve from the memory monitor oscilloscope, or the data can be read out of the analyzer memory by a paper strip printer, a magnetic tape unit, or by a Teletype printer. When the data sets are in the magnetic tape or Teletype paper tape formats, the data can be directly read into a computer for processing and plotting.

Single Photon Detection System

The purpose of the single photon detection system described below was to detect the light emission from suspensions of Scenedesmus algae. The red fluorescent light from the algae passed through a 690 nm interference filter to eliminate the 488 nm laser stimulus light. An iris limited the fluorescent light to an intensity range suitable for the photomultiplier.

Due to the 50-ohm load resistor in the photomultiplier base assembly, the photomultiplier output signal consisted of a population of discrete pulses of low voltage amplitudes which were superimposed on a stable zero voltage baseline. In the photomultiplier tube's linear range of operation, the number of pulses per second was proportional to the light intensity striking the photocathode of the photomultiplier tube.

The photomultiplier tube's output pulses were amplified sixteen fold to one hundred fold, as appropriate for the input light signal, by 50-ohm low noise amplifiers and then fed to a discriminator which eliminated the lower amplitude "noise" pulses of the photomultiplier tube's output signal and reshaped each of the higher amplitude pulses into pulses of uniform voltage amplitude and duration.

The detection system was assembled so as to have maximum sensitivity to the fluorescence light from the algae, and also to have a minimum noise level. Thus, it was imperative to prevent the system's accidental detection of impulse-type (digital) noise from outside sources. This demanded electrical shielding of the photomultiplier tube and base assembly.

Refer to Figure 1 for the instrumentation schematic diagram and associated symbols of the detection system. The photomultiplier tube[1], an Amperex 56CVP, and its base assembly (PMS) were inserted into a plastic pipe which traversed the interior of an aluminum-covered light-tight insulated box (BOX2). The inside perimeter of this box was well insulated with styrofoam. The interior central portion of the box surrounding the photomultiplier tube's plastic pipe contained a plastic-lined vacant space which could be

---

[1]Amperex Electronic Corp., Hicksville, New York 11802.

Figure 1. Schematic diagram of the instrumentation for photon-counting experiments which utilized the rotating disc for laser beam modulation. ADC, analog-to-digital converter; AIL, Argon-ion laser; A,P1 and AMP2, 50-ohm quad amplifier module; BOX1, wooden light-tight enclosure; BOX2, electrically shielded, thermally insulated box; CL, recollimation lens; CU, coincidence unit; DISC1 and DISC2, discriminator, dual unit module; FET, photo field effect transistor; FL, 690 nm optical interference filter; FS, aluminum foil strip; HNL, Helium-Neon laser; NVS, high voltage supply; IR, iris; LF, focusing lens; MC, memory control unit; MEM, memory array and driver unit; MO, microscope objective lens; MS, beam splitter; PD, photodiode; PM, photomultiplier tube; PMS photomultiplier tube socket and base assembly; PR, Teletype printer; PU1 and PU2, square wave pulse units; RD, rotating disc; RIO, read-in/read-out module; SC, memory unit monitor scope; TAC, time-to-amplitude converter.

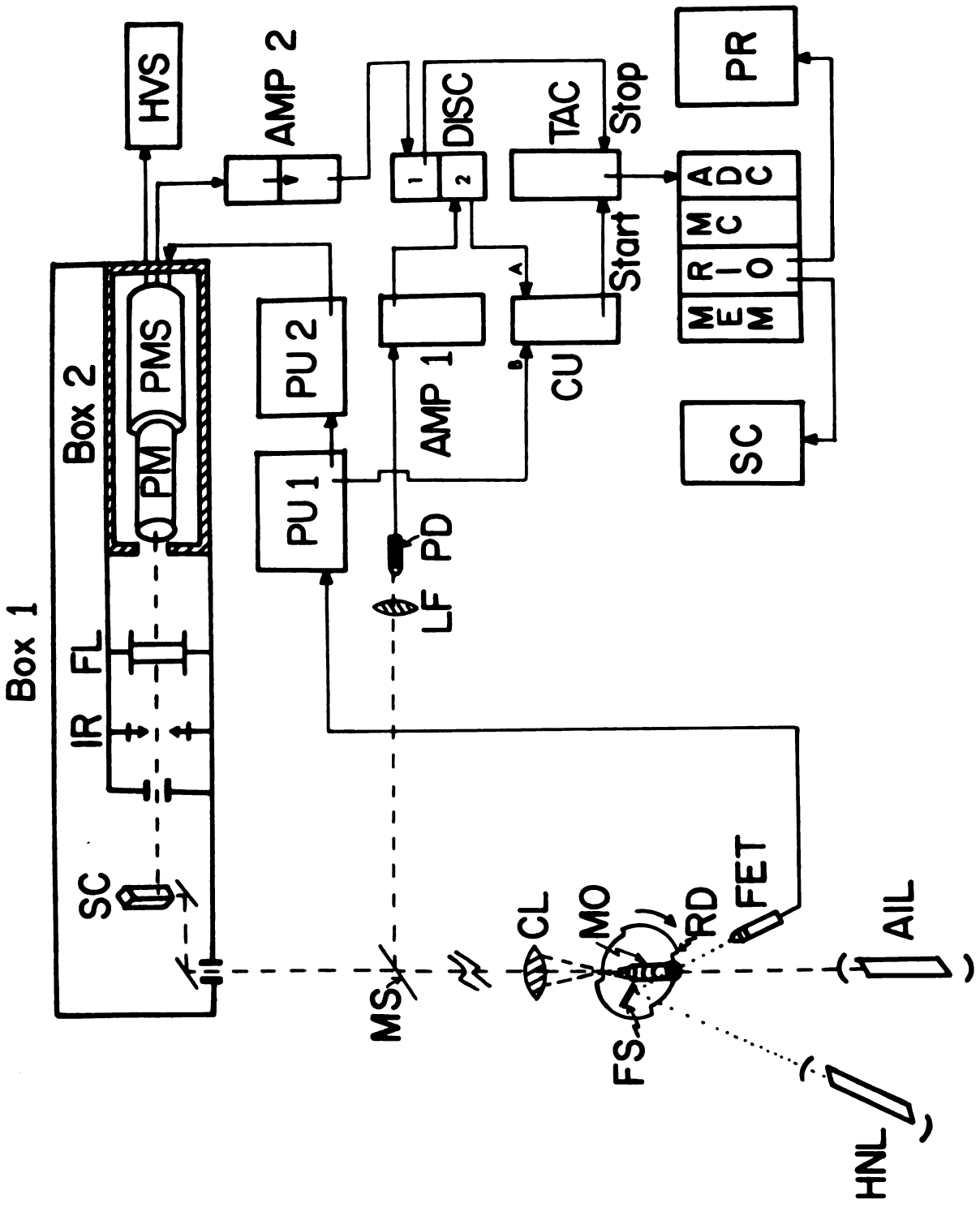
HVS
AMP 2
DISC
TAC
Stop
PR
Box 2
PMS
PM
PU 2
AMP 1
CU
Start
MEMORY
ADC
SC
PU 1
PD
LF
Box 1
IR
FL
SC
MS
CL
MO
RD
FET
AIL
FS
HNL

packed with dry ice fragments. The cooling of the photomultiplier tube and base assembly to dry ice temperature greatly reduced the thermal noise of the detection system.

The output from the photomultiplier socket was amplified 16 to 100 fold by a series of low noise 50-ohm amplifiers[2] (AMP2), and then connected to the discriminator[3] (DISC1) input. The input discriminator's rejection level was adjustable from 5 mV to 1 V by means of a front panel ten-turn potentiometer.

The high voltage supply[4] (HVS) for the photomultiplier base assembly and the discriminator input level control were two parameters which had to be adjusted to achieve linearity for the light detection system. The adjustment scheme was to count the frequency of the discriminator output pulses by a high speed counter while neutral density filters were placed between a constant intensity light source and the photocathode. The photomultiplier high voltage source was adjusted slightly about the -1500 V level, and the discriminator input level control also varied about its lowest setting so as to obtain a set of conditions in which the discriminator output rate was linear with light intensity.

---

[2]Model 104, Keithley Instruments, 28775 Aurora Road, Cleveland, Ohio 44139.

[3]Model T105/N, EG&G Nuclear Instrumentation Division, 35 Congress Street, Salem, Mass. 01970.

[4]Model 246, Keithley Instruments, ibid.

An adjustable iris (IR) was always used in the path of the algal light emission from the algal sample to the photomultiplier tube photocathode. The iris was centered in the two-inch diameter pipe leading toward the photomultiplier tube enclosure. The iris aperture was adjustable so as to attenuate any incoming light intensity to those orders of magnitude which the photomultiplier detector system could measure.

Photomultiplier Tube Gating Circuit

A photomultiplier tube gating circuit was designed for use with the 56CVP photomultiplier tube in the single photon counting instrumentation. The photon counting system was designed to measure the delayed light emission from Scenedesmus algae during experiments in which the algal sample was illuminated by the modulated laser beam. The algal sample emitted a strong fluorescence during the illumination interval of each laser light modulation cycle. Immediately after the laser beam was extinguished by the light modulator, the delayed light emission was measured. A gating circuit was desired for the photomultiplier tube which would maintain the photomultiplier tube at low sensitivity for most of the light modulation cycle and then bring the photomultiplier tube to high sensitivity at the instant the laser beam was extinguished at the sample site.

For some experiments, it was desired that the gate circuit hold the photomultiplier tube at full sensitivity for 100 microseconds or longer after each laser flash.

The systems for photomultiplier tube gating which are described in the literature were not useful for the above biological experiments. Circuits are designed for momentary high efficiency cutoff of a photomultiplier tube sensitivity (59), while other circuits are designed to turn on a photomultiplier tube's sensitivity briefly (60). These circuits provide control of the phototube sensitivity only for a small duration of time, usually less than 20 microseconds.

The unique feature of the gating circuit described here is the use of an electro-optical GaAs diode-phototransistor coupler. This semi-conductor device allows an electrical isolation of 2500 VDC between the gate signal to the gating circuit and the tube base assembly switching transistor. The coupler also allows the use of a gate signal pulse of virtually any duration, i.e., from microseconds to minutes. The gate signal input to the coupler need be only + 2 V amplitude pulses. The gate signal generator can therefore be an economical low voltage pulse unit.

The schematic diagram of the gating circuit is presented in Figure 2. The 2N5416 PNP transistor acts as a

Figure 2. Schematic diagram of the gating circuit for the 56CVP photomultiplier tube.

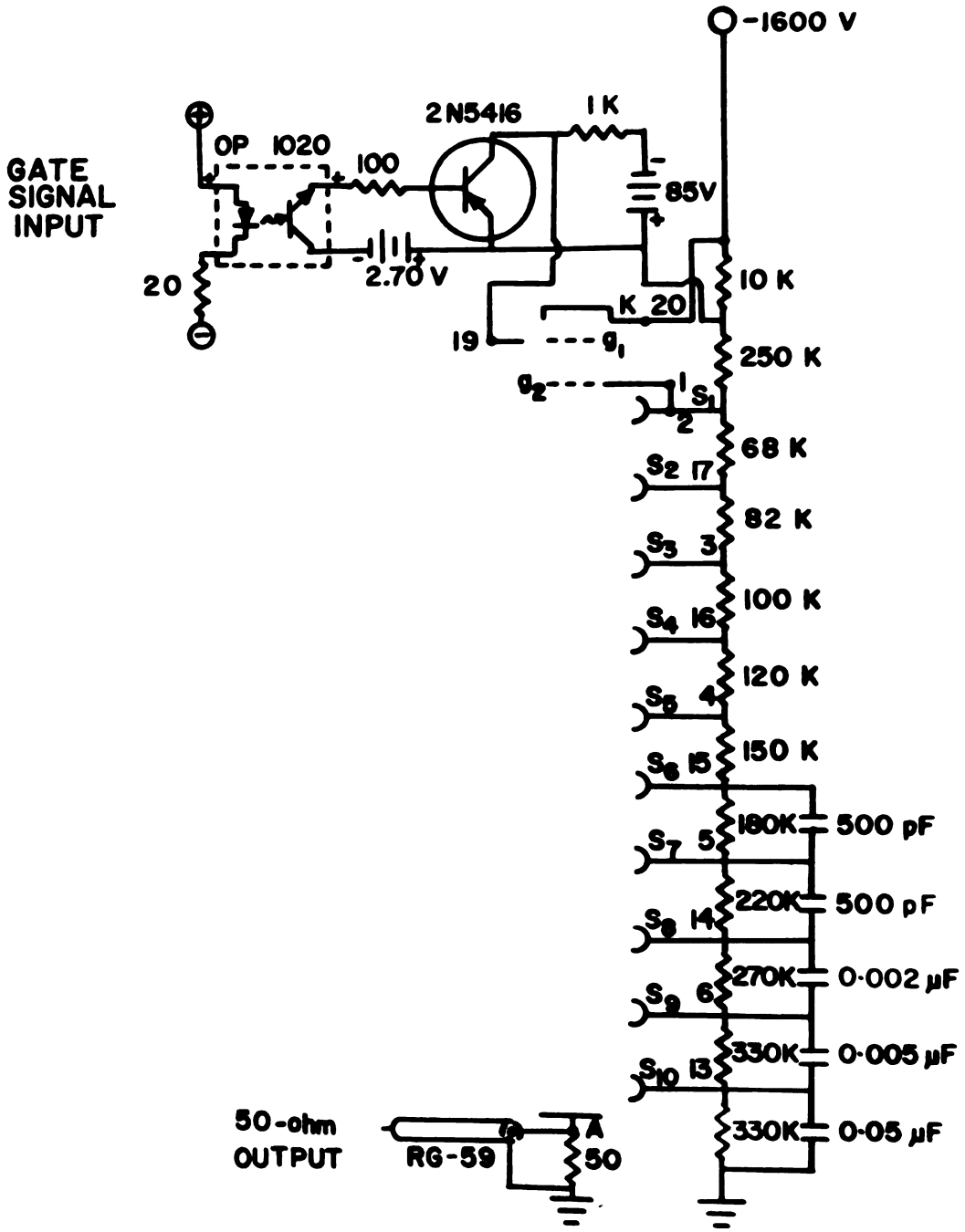
-1600 V
GATE SIGNAL INPUT
OP 1020
2N5416
1 K
100
85V
2.70 V
20
10 K
K 20
19
g_1
g_2
250 K
S_1
2
68 K
S_2 17
82 K
S_3 3
100 K
S_4 16
120 K
S_5 4
150 K
S_6 15
180K
500 pF
S_7 5
220K
500 pF
S_8 14
270K
0·002 µF
S_9 6
330K
0·005 µF
S_{10} 13
330K
0·05 µF
50-ohm OUTPUT
RG-59
A
50

high voltage switch and controls the voltage of the 56CVP photomultiplier tube focusing electrode. When the 2N5416 transistor is not conducting, the focusing electrode is maintained at 85 V negative with respect to the photocathode. In this case, the photomultiplier tube is insensitive to light. When the 2N5416 conducts, the potential of the focusing electrode falls to the same voltage level as the photocathode. The phqtomultiplier tube then has much greater sensitivity.

The base of the 2N5416 transistor is controlled in turn by the electro-optic coupler device[5]. This unit consists of a Gallium-Arsenide light emitting diode (LED) and a Silicon phototransistor. Both elements are enclosed by a moulded black plastic housing. The lens of the LED faces the phototransistor lens with an electrically insulating air space between them. The LED emitter element of the coupler unit is driven by a low voltage pulse generator having a 50-ohm output (PU2). The phototransistor detector element of the coupler unit is connected in series with a small battery, a resistor, and the base of the 2N5416 switching transistor. When no gate signal is present, there is no current flow through the LED emitter. The detector phototransistor then acts as a high resistance and

---

[5]Coupler Unit OP1020, Optron, Inc., 1201 Tappan Circle, Carrollton, Texas 75006.

prevents current flow through the 2N5416 base. The 2N5416 does not conduct and the photomultiplier tube is maintained at very low sensitivity. When the LED emitter is driven by a positive 2 V pulse gate signal, the LED emitter of the coupler unit emits infrared light toward the photo-transistor half of the coupler unit. The phototransistor then acts as a short circuit element in the 2N5416 base circuit. Current can then flow through the 2N5416 base from the small 2.7 V mercury battery, causing the 2N5416 to conduct. As long as the 2N5416 conducts, the photo-multiplier tube has maximum sensitivity.

The 85 V battery for the 2N5416 transistor was formed of seven 12.15 V pen-light sized batteries connected in series. The seven batteries were packed together side by side in the interior region (5" long x 2.5 " diameter) of the photomultiplier tube base assembly. The batteries were held in place in the base assembly by two circular fiber board insulators. The insulator boards had been predrilled with a centered hexagon pattern of holes with a drill which corresponded to the diameter of the batteries.

The gate signal was brought into the base assembly through a 50-ohm RG-58 cable from the 50-ohm output con-nector of the low voltage pulse unit (PU2). The 50-ohm cable was terminated at the base assembly in a polarized two-pin Jones plug. Two short wires led from the Jones plug directly to the input of the electro-optic coupler.

The coupler, the 2N5416 switching transistor, and all the other components were mounted on a ceramic terminal strip which was in turn mounted on the interior side of the metal end plate of the socket base assembly.

The switch-on time for the circuit in Figure 2 was four microseconds for 100% turn-on. Faster turn-on could probably be accomplished by redesigning the circuit for a diode-diode electro-optic coupler unit with a turn-on time of 30 nanoseconds.

The photomultiplier tube and base assembly were cooled with dry ice during operation. The circuit of Figure 2 worked well under these conditons.

Source and Modulation of Stimulus Light

In all experiments of this thesis, an Argon-ion laser[6] (AIL) served as the algal stimulus light source. The steady light beam from the laser was modulated on and off in a repetitive fashion, and the light emission was measured from the algae during the microseconds following the instant the laser stimulus light was switched off at the algal sample site. At the end of every stimulus light modulation cycle, a reference electronic pulse was generated by accessory electronic circuits at the instant the laser

---

[6]Model 54 Argon-Ion laser, Coherent Radiation, 932 East Meadow Drive, Palo Alto, California 94303.

beam was switched off at the algal sample. All timing in each experiment was measured in relation to this (t = 0) reference pulse.

The Argon-ion laser was operated with the wavelength selector prism in place, selecting the 488 nm wavelength emission. The output power of the laser was about 120 mW/cm^2 when the laser was operated at the 488 nm wavelength. The algae eventually received about 18 to 25 mW/cm^2 at the algal sample site, the attenuation of the beam resulting from the 50% duty cycle modulation of the laser beam by the modulation device and scatter from three first surface mirrors which directed the beam to the algal sample holder site.

Two methods of on-off modulation of the laser beam were employed in experiments of this thesis. When it was desirable to achieve an extinction of the stimulus laser beam at the sample in the range of 20 nanoseconds, an electro-optical modulator (Pockel's cell) was utilized. When an extinction of the laser light within 250 nanoseconds was satisfactory, a rotating disc, with opposing ninety degree sectors passing the light beam, was used.

Rotating Disc Laser Modulator

Figure 1 shows the schematic diagram of the instrumentation used in a typical experiment with the laser light beam being modulated by the rotating disc apparatus. The collimated light of the laser beam passed through a five

power microscope objective lens (MO) which focused the beam to the point where the beam was chopped by the rotating disc (RD). The modulated diverging light was collected by the one inch diameter lens (CL) which recollimated the laser light. The recollimated chopped beam was routed by mirrors to the interior of a light-tight box (BOX1) which surrounded the sample holder, the sample cuvette, and the photomultiplier tube.

The speed of the electric motor[7] which spun the rotating disc was controlled by a 1 kW, 117 VAC variable autotransformer. Most experiments used a 75 VAC output from this autotransformer. With the motor turning the disc at 250 Hz, and with the Argon laser beam passing through the open sectors of the rotating disc, the five-power microscope objective lens was positioned horizontally in the laser beam close to the rotating disc. The objective lens was moved horizontally toward the rotating disc by means of a rack and pinion device. At the same time, an oscilloscope displayed the voltage output of a photodiode[8] (PD) which had been placed in the path of a reflected portion of the chopped laser beam. It was possible to adjust the microscope lens to a point where the laser light beam was chopped at the

---

[7]Model NSE-13, Bodine Electric Co., 2500 W. Bradley Place, Chicago, Ill. 60618.

[8]Source-gate junction of FET phototransistor FF108, Crystalonics, 147 Sherman Street, Cambridge, Mass. 02140.

focus point in 225 to 250 nanoseconds when the motor was rotating the disc at 250 revolutions per second. For the 90-degree sector rotating disc, the resulting laser beam modulation pattern was one millisecond durations of alternating dark and light periods.

The photodiode (PD) output square wave voltage was amplified four fold by a 50-ohm amplifier[9] (AMP2) and fed to a discriminator unit[10] (DISC2). The discriminator unit was adjusted to produce an output pulse only on the very early negative slope of the square wave output from the photodiode. This slope corresponded to the instant the Argon laser beam was chopped by the rotating disc. The discriminator output pulse defined the instant the laser light beam was extinguished. The photodiode operated in the photovoltaic mode.

A second trigger signal was generated for use in coincidence with the photodiode trigger signal. The two signals in coincidence mode provided a most reliable trigger signal which had less than 50 nanoseconds variation about the instant of light extinction. This second trigger signal was generated by placing a narrow aluminum foil strip (FS) radially on the black anodized surface of the rotating

---

[9]Model AN201/N, EG&G, ibid.

[10]Model T105/N, EG&G, ibid.

disc and then illuminating the rotating disc surface with the beam from a 1 mW/cm^2 He-Ne laser[11] (HNL) such that the small foil strip traversed the fixed He-Ne laser beam once each revolution of the disc. A FET phototransistor[12] (FET) was positioned within a centimeter of the rotating disc surface at the proper angle to catch the He-Ne laser beam reflected from the foil strip as the foil strip moved through the laser beam.

The phototransistor (FET) output pulses were used to trigger a small electronic square wave pulse unit[13] (PU1). The width of the output pulse from this unit was synchronized so as to overlap in time the discriminator output pulse of the photodiode (PD) which was described above. A dual beam oscilloscope was used to speed this adjustment procedure.

The square wave pulse unit (PU1) signal and the discriminator output signal were connected to the inputs of a coincidence module[14] (CU). This unit produced an output pulse only when both the pulser's output pulse and the photodiode discriminator pulse were in coincidence. The coincidence pulse was then regarded as the true t = 0 pulse.

---

[11]Model 133, Spectra-Physics, Mountain View, California.

[12]FF108 FET phototransistor, Crystalonics, ibid.

[13]Model 8003A, Hewlett-Packard, 1501 Page Mill Road, Palo Alto, California.

[14]Model C104/N, EG&G, ibid.

The triggering scheme was discussed above in detail because it was essential to have a stable t = 0 reference signal which had no "jitter" in relation to the instant of each individual laser light extinction in order to take full advantage of the 250 nanosecond stimulus light extinction. The above scheme always produced a reference signal on only one sector of the two-sector rotating disc. The discriminator units and the coincidence unit were nuclear instrumentation timing modules with individual timing errors of less than one nanosecond. Therefore, any timing error in the t = 0 reference signal in relation to the laser light extinction was due to voltage change in the photovoltaic output waveform from the photodiode.

Electro-optical Laser Modulators

The electro-optical Pockel's cell type of laser beam modulator[15] was used when it was desirable to switch off the stimulus laser light beam at the algal sample in the range of 20 nanoseconds. The electro-optical laser modulator was used only in experiments in which the pulse-height analysis system of photon counting was used. Only the pulse-height analysis system had fast enough time resolution to take advantage of the nanosecond light modulation of the electro-optical laser light modulators. When in operation at 50 Hz

[15]Model EOLM-400 modulator, ISOMET, Corp., 433 Commercial Avenue, Palisades Park, New Jersey 07650.

repetition rate, the electro-optical modulators' electronic driver unit[16] passed a high voltage to the electro-optical light modulator units for 15 milliseconds of each modulation cycle, causing the modulator units to pass the laser beam with minimum attenuation. When the high voltage was relaxed, the laser light beam was extinguished for the remaining five milliseconds of each modulation cycle. One fault of the electro-optical modulator system was that there was apparent some sort of resonance effect in the modulation crystal, or an oscillation in the electronic drive circuit which allowed a small amount of the light beam to again pass through the modulator some two or three microseconds after the modulator had switched the laser beam off. This phenomenon prevented the electro-optical modulator system from being used in all experiments except those in which only the delayed light emission of the algae was to be measured in the first few microseconds following stimulus light extinction. The rotating disc modulator system was used for experiments with photon counting over intervals longer than two microseconds.

Before beginning an electro-optical modulation experiment, the mechanical rotating disc apparatus was removed from the laser beam path. The polarizers were installed and

---

[16]Model HVQ-2X4105 High Voltage Pulse Generator, ISOMET/electronics, 5414 Port Royal Road, Springfield, Va. 22151.

adjusted for extinction of the laser beam. The electro-optical laser modulators were then moved to their positions between the polarizers. The modulators were mounted in double gimbal suspensions[17] which allowed precise adjustment of the modulators' position and orientation in the laser beam. An oscilloscope displayed the photovoltaic signal from a photodiode in the modulated laser beam during the adjustment of the modulator's orientation in the laser beam. The modulator was adjusted for best contrast ratio, i.e., for maximum light transmission in the "light-on" period, and minimum light transmission in the "light-off" period of the light modulation cycle.

In order to achieve a much higher contrast ratio, two electro-optical modulators were used in series in most of the experiments which utilized the electro-optical method of modulation. Three polarizers were used in this case, with the extra polarizer positioned between the two modulators. The two modulators had to be adjusted individually. This was accomplished by either removing one of the modulators from its position in the laser beam path, or by compromising the modulation of one modulator by means of a quarter wave plate properly positioned in the laser light

---

[17]Model AOB 10.503, Lansing Research Corp., 705 Willow Ave., Ithaca, New York 14850.

beam next to the modulator exit aperture.

The laser beam polarizers were of the calcite crystal type, having extinction ratios of 10^6:1. Both the cemented and the air-gap spaced models of the Thompson polarizer were found to be satisfactory.

In experiments in which the electro-optical modulation was used, the electronic t = 0 reference timing signal had to be generated in a different manner. A square wave pulse generator was adjusted to 50 Hz to serve as the basic timing oscillator. The 50 Hz output pulses of this unit were distributed, in parallel, to several precision time-delay units[18]. The time delays of these units were adjusted, as needed, to trigger the monitor oscilloscope sweep trigger input, the pulse-height analysis instrumentation, the pulse input of the laser light modulator drive unit, and, when used, the photomultiplier gating system. The laser modulator driver unit produced an output trigger signal several hundred nanoseconds before each switching cycle of the laser light, and this trigger signal could be monitored in order to detect any jitter in the various time delay circuits.

---

[18]Model 437A, ORTEC, Inc., 100 Midland Road, Oak Ridge, Tenn. 37830.

Pulse-Height Analysis System

The pulse-height analysis system was utilized as the signal processing system in those experiments which measured the nanosecond and microsecond components of the algal delayed light emission. The following paragraphs describe the operation of the pulse-height analysis system, as used in the experiments of this thesis.

The complete set of components necessary for a pulse-height analysis experiment is shown in Figure 1. The light detection system and the elements of the light modulation system have already been described. The pulse-height analysis signal processing system consisted of the time-to-amplitude converter[19] (TAC), the analog-to-digital converter[20] (ADC), and the multichannel analyzer[21] (MCA).

The output pulses from the light detection system (from discriminator DISC1) were fed to the TAC, together with the t = 0 timing signal pulse which was generated each stimulus light modulation cycle. The method of generation of the t = 0 timing signal has already been described in this instrumentation chapter. The algal light emission detection

---

[19] Model 437A, ORTEC, Inc., ibid.

[20] ADC, Series 2200 Instruments, Nuclear Data, Inc., P.O. Box 451, Palatine, Ill. 60067.

[21] Series 2200 Instruments: Master Control Unit, Read-in/Read-out Unit, and Memory Driver Unit, Nuclear Data, Inc., ibid.

system has also been described previously in this chapter. The TAC instrument produced an output pulse which was proportional in voltage amplitude to the time interval which elapsed between the arrival, at the TAC "start" cable input, of the t = 0 timing signal and the arrival, at the TAC "stop" input, of the first of the few pulses from the light detection system discriminator DISC1. Only one TAC output pulse could be produced each light modulation cycle, because the internal timing circuit of the TAC was triggered only by the t = 0 reference signal which occurred once each stimulus light modulation cycle. Thus, the TAC clocked the arrival of the first pulse from the discriminator DISC1 and produced an analog voltage output proportional to the clocked interval. One should appreciate that the operation of the TAC was based on the timing of arrival of photomultiplier tube pulses which have been discriminated and reshaped and not on variations in photomultiplier tube output current.

The analog output pulses from the TAC were routed to the input of the analog-to-digital converter (ADC). After the TAC produced an output pulse, the ADC processed the pulse according to the pulse's voltage amplitude and then produced one count in the proper channel of the multichannel analyzer. The channel numbers had been previously calibrated as a time axis. As the repetitive modulation cycles of the laser light caused the algae to produce an amount of delayed

light emission each modulation cycle, more and more data counts accumulated in the multichannel analyzer memory array. A histogram was eventually formed by the data. This histogram represented the intensity of fluorescent light from the algae (represented by the number of data counts per channel) as a function of time (represented by the set of channel numbers).

The linearity of operation of the TAC, the ADC, and the MCA was checked for each time range of the TAC. The ADC input controls were adjusted so that a plot of MCA channel number as a function of time of delay of the TAC stop pulse produced a straight line which passed through the origin of the plot. Each of the time ranges of the TAC was precalibrated in this manner by feeding into the TAC pulse pairs separated by known delay intervals and recording the resulting storage channel number in the MCA system. All ADC control settings and TAC calibration curves were recorded and saved for later reference.

After this calibration procedure, the channel numbers of the MCA could be labelled as points along the time axis for any TAC data recorded in the MCA memory array. The TAC start pulse served as the origin point for this time axis.

If the photomultiplier/discriminator light detection system had a linear output with intensity, the ordinate of the MCA display histogram could be labelled as "relative light intensity".

The operating conditions for the pulse-height analysis apparatus were determined before attempting a pulse-height analysis experiment with the algae. First, special care was taken so as not to overexpose the photomultiplier tube. The photomultiplier tube output signal was monitored on an oscilloscope while the iris protecting the photomultiplier tube aperture was slowly opened. The iris was never opened beyond the point where the baseline of the photomultiplier tube output did not remain flat and undistorted, as viewed on the oscilloscope. A cuvette filled with an acetone solution of chlorophyll provided a convenient control light signal which had a fluorescence component at 690 nm but no delayed light emission. Second, the count rate of the TAC was adjusted while the chlorophyll-acetone solution fluorescence light signal was supplemented by a low intensity unmodulated signal. The low intensity light signal simulated the delayed light emission of the algae while the adjustments of the electronics were completed. The TAC count rate was adjusted to as high a rate as possible, but not exceeding the rate at which the low intensity unmodulated light signal was recorded as anything but a straight horizontal line on the MCA memory monitor scope. Since the TAC start pulses occurred at the fixed rate of the light modulation frequency, the rate of the TAC stop pulses had to be reduced when the TAC count rate was too high by again reducing the aperture of the iris.

Recording of Waveform of Electro-optical Modulation

The following paragraphs describe the instrumentation used to record the exact waveform of the laser light extinction by the electro-optic modulators. The light detection element was a photodiode placed in the modulated laser beam. The diode produced a photovoltaic voltage in proportion to the light intensity striking the diode. In order to record and measure this diode voltage waveform over a five microsecond time interval about the instant of stimulus light extinction, the diode signal was amplified and displayed by a sampling scope which was hooked in turn to the signal averager module of the multichannel analyzer. A cable connected the photodiode to the 50-ohm input ampifier of a 4S1 sampling unit of a Tektronix 661 sampling scope. The digital output amplifier of the sampling scope was connected to the input of the signal averager module. Figure 3 shows the wiring scheme for the connection of the sampling scope to the MCA. Both the sampling scope and the MCA were triggered by the same trigger signal. The trigger signal was synchronized to occur each stimulus light modulation cycle some 1.5 microseconds before the instant of light extinction. The sampling scope sweep was exactly synchronized to and controlled by the signal averager sweep. Therefore, the photodiode signal, which was displayed on the sampling scope, was sampled in unison with the sweep of the signal averager.

Figure 3. Schematic diagram of the instrumentation used in the recording of the stimulus light extinction by the electro-optical laser modulators. Pulse Unit, Hewlett Packard Model 1900; MD1 and MD2, Electro-optical modulator drive units; M1 and M2, Electro-optical laser beam modulators; P1, P2, and P3, Calcite prism polarizers, 1-cm square aperture; Diode, Gate-source junction of FET phototransistor; 661 Scope, Tektronix 661 Sampling Scope with plug-in units; SA, Signal averager module of the multi-channel analyzer; R-I-O, Read-in/read-out module of the multichannel analyzer; ARL, Argon-ion laser.

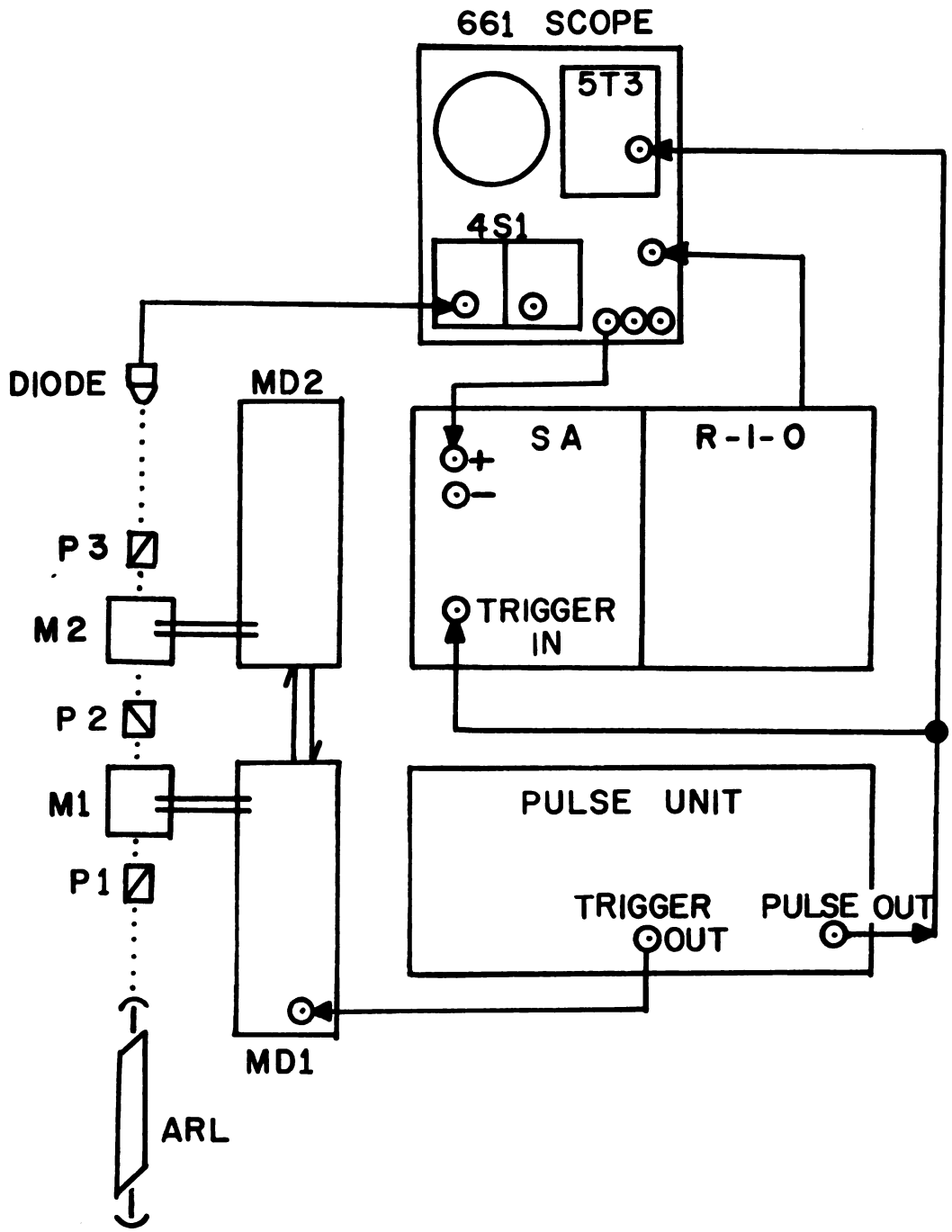
661 SCOPE
5T3
4S1
DIODE
MD2
SA
R-I-O
+
−
P3
M2
TRIGGER
IN
P2
M1
PULSE UNIT
P1
TRIGGER
OUT
PULSE OUT
MD1
ARL

The digitized photodiode signal resulting from the sampling process was the signal which was recorded by the signal averager. One hundred to two hundred sweeps of the signal averager were enough to record the photodiode signal waveform.

Recurrent Multiscaling

Whenever it was necessary to measure decay curves over time intervals greater than a few hundred microseconds, the recurrent multiscaling mode of the MCA was used. The recurrent multiscaling mode of operation was selected by switching the MCA mode switch from the pulse height analysis (PHA) position to the recurrent multiscaling (MS RECUR) position. When the mode switch was switched from PHA to MS RECUR, control of the addressing of MCA channels was changed from the analog-to-digital converter module to the internal circuitry of the MCA itself. The ADC achieved random addressing into the MCA memory array during pulse-height analysis experiments. However, when the MCA operated in the MS RECUR mode, the entire preselected set of MCA channels were "swept", i.e., the channels were individually addressed electronically in sequence, from the lowest numbered channel up through the highest numbered channel.

The sweep cycle of the MS RECUR mode was initiated by a single trigger pulse arriving at the MS "start" input BNC connector on the front panel of the MCA master control module.

With the MS RECUR mode, each multiscaling sweep was initiated by the phototransistor trigger pulse from the rotating disc modulator. The trigger pulse was synchronized to occur fifty microseconds before the end of the laser light flash at the algal sample.

During recurrent multiscaling experiments, the photomultiplier tube, amplifiers, and discriminator of the light detection system were operated in the same manner as for the TAC experiments. However, the output pulses from the photomultiplier tube discriminator had to be electronically "stretched" in duration and amplified to six volts amplitude so that they could properly toggle the MS "count" BNC input circuit of the MCA. The discriminator pulses that were originally seven nanoseconds in duration were stretched to durations of 60 nanoseconds by means of connecting a 30-foot length of RG-58 cable to the width BNC connectors of the EG&G discriminator. The stretched pulses were amplified by the channel # 1 amplifier of a 1A1 dual trace plug-in unit of the Tektronix RM547 oscilloscope. The amplifier gain was set to 0.1 V/cm. The amplified and stretched pulses from the photomultiplier output discriminator were then routed from the channel # 1 amplifier output BNC connector to the MS count input BNC on the MCA.

Each stretched discriminator pulse arriving at the MS count BNC of the MCA during a sweep of the MCA was added as a single count to the count total of whichever channel

was aquiring at the instant the pulse arrived at the MCA. Thus, during the course of a multiscaling experiment, all pulses arriving at the MCA count BNC were automatically sorted into the proper MCA channels, depending on the time of arrival of each pulse during a recurrent multiscaling cycle.

An internal clock of the MCA was preset for the desired dwell time per channel, 20 microseconds. The dwell time value determined the time interval between the activation of adjacent channels during the multiscaling sweeps of the MCA memory. The total time for one complete sweep of the MCA was simply the product of the dwell time per channel times the number of channels in each sweep cycle. Since all channels had the same dwell time, they represented discrete time increments along a time axis which had its origin at the instant of the trigger signal which initiated the recurrent multiscaling sweep. Since the phototransistor trigger signal was always synchronized to the end of the light flash at the sample site, the recurrent multiscaling sweep cycles repetitively occurred over the same time interval following the end of the light flashes. Thus, the MCA channels could be identified as specific points along the time axis following stimulus light extinction. The totals of counts in the MCA channels eventually formed a decay curve which represented the decay of light emission from the algae. The data could be

normalized and plotted as "relative intensity" as a function of "time". The decay curve could be photographed directly from the MCA monitor oscilloscope or the data could be read out of the MCA via a Teletype read-out unit.

Single Sweep Multiscaling System

The last set of experiments of this thesis used the single sweep multiscaling mode of the multichannel analyzer. This mode of operation resembled the recurrent multiscaling mode in that the digital information from the detection system was fed directly to the multiscaling input connectors of the MCA. The single sweep multiscaling mode differed from the recurrent multiscaling mode in that there was no trigger signal necessary for the MS "trigger" input connector because only one slow sweep of the 1024 channels of the MCA was used.

The purpose of the last set of experiments of the thesis was to measure only the changes in the first 60 microseconds of the delayed light emission from the algae, i.e., to electronically segregate and count only the photomultiplier tube output pulses that occurred during the first 60 microseconds following each stimulus light modulation cycle. This was accomplished by operating the photomultiplier tube output discriminator, DISC1, in the gated mode, i.e., the discriminator's mode toggle switch was moved to the "gate" mode and an external gate signal pulse of + 5 V

amplitude was applied to the gate input connector of the discriminator. The leading edge of the gate signal was adjusted so as to occur five microseconds after the instant of the light extinction at the algal sample.

The output pulses of the gated discriminator were stretched, amplified, and applied to the count input BNC of the MS section of the MCA as described above in the section on recurrent multiscaling mode instrumentation.

The MCA dwell time clock was set to 0.8 seconds per channel and all 1024 channels of the MCA were used in each experiment. Only one sweep of the MCA was used to record the variation in rate of the photomultiplier tube pulses of the gate period during the first 820 seconds of the induction period. The MCA mode switch was moved from the MS RECUR position to the MS position, and the "start" BNC input connector of the MS section of the MCA was grounded by a shorted BNC plug. This grounded BNC plug allowed initiation of the multiscaling single sweep when the MCA was switched to "aquire". The high speed rotating disc apparatus was used to chop the laser beam, and the photo-transistor trigger signal of the rotating disc apparatus was used to trigger the pulse unit providing the gate signal for the gated discriminator.

METHODS

The methods chapter of this thesis describes three different experimental conditions under which the delayed light emission was recorded from the algae. The so-called steady-state condition was that in which the delayed light was measured after the algal sample had been preilluminated by the modulated stimulus laser light for thirty minutes. The so-called induction condition was that in which the delayed light was measured during the light induction period of dark-adapted algal samples. The light induction period was described previously in the introduction chapter. The third set of experimental conditions, called the flow conditions, was that in which the delayed light emission was measured during the first second of exposure of the dark-adapted algal sample to the modulated stimulus laser light.

This methods chapter of the thesis is divided into five sections. The first section describes the culture of the algae and the experimental procedures for establishing the three experimental conditions. The second section of

the chapter describes the procedures of the experiments which utilized the pulse-height analysis mode of photon counting to measure delayed light under both steady-state and flow conditions. The third section of this chapter describes the procedures which were used to estimate the ratio of prompt fluorescence intensity relative to the first microsecond of delayed light emission. The fourth section of this chapter describes the procedures of the experiments which utilized the recurrent multiscaling mode of photon counting to measure the delayed light under flow and induction conditions. The final section of this chapter describes the experimental procedure of the experiments which utilized the single sweep multiscaling photon counting mode to measure delayed light under the induction conditions.

Culture of Algal Strains

The D_3 wildtype strain of Scenedesmus obliquus algae was grown in 250 ml glass flasks under constant illumination from four 40 W "cool white" fluorescent bulbs. The bulbs were at a distance of 18 inches above the flasks. A small diameter air hose distribution system delivered a constant stream of filtered air, enriched 2% with CO_2 gas, to the metal cap of each flask. The gas mixture was fed to the bottom of a flask by a small length of glass tubing inside the flask. The glass tubing was connected to the air inlet of the flask metal cap by a short length of rubber tubing.

The flasks stood on a shaker machine which maintained the contents of the flasks in constant agitation.

Stocks of the Scenedesmus mutant number 8 were grown in the dark on refrigerated agar slants. The algae were transferred from the slant cultures into 10 ml of Bishop's media (61), supplemented with 0.5% glucose and 0.025% yeast extract (62). The liquid cultures were grown in the dark, on the shaker machine, at room temperature.

Steady-State Conditions

The experimental procedure for the steady-state experiments was to harvest the algae culture, prepare the sample algal suspension, and allow the sample to achieve steady-state conditions of illumination by placing the cuvette containing the algae in the modulated laser beam in the sample holder thirty minutes before the beginning of the experiment. The one centimeter square quartz cuvette was filled to two thirds full volume with the algal suspension. A Teflon stopper for the cuvette was pierced with two holes. One hole admitted a hypodermic needle through which the air mixture passed. The second hole held a second hypodermic needle which served as the air vent.

Flow Conditions

The wildtype algae were harvested and resuspended in growth media to the proper concentration. The wildtype

algae were allowed to dark-adapt during two hours of darkness inside a foil wrapped flask. The mutant 8 algae were retained in their dark-adapted growth state during harvesting and dilution to proper concentration with fresh growth media. All handling of the algae was done with all room lights extinguished except for the indirect illumination from one 20 W incandescent bulb some twenty feet away from the apparatus. A flow system was devised which moved the suspension of dark-adapted algae through the stimulus laser beam at the rate of 1 ml/sec. The delayed light emission was measured during the instant the algae passed through the modulated light beam.

The flow experiments were performed while a four-liter flask of algal suspension drained by gravity through a six-foot length of surgical tubing to a lower reservoir. The flask was wrapped in foil and the mouth of the flask was capped with foil which fit over the rubber tubing siphon. Immediately before an experiment, the flow of algal media was started by suction and the flow rate was adjusted to the proper value. The tubing from the flask was routed into the light-tight box which surrounded the cuvette holder, the photomultiplier tube's insulated box, and the holder for the 690 nm optical filter and iris mechanism. The cuvette holder was removed and replaced by an eight-centimeter length of quartz tube of 9 mm diameter.

The section of the quartz tube was held vertically by ring-stand clamps. The surgical tubing was cut, and the length of quartz tube inserted between the two cut sections. The modulated laser beam was reoriented so as to horizontally intersect the quartz tube at the point exactly in front of the photomultiplier tube iris. During the experiments, the algal suspension flow was adjusted with a tubing clamp on the tubing close to the drain reservoir. The flow rate was adjusted for a one-inch per second flow of algal cells along the tubing, i.e., about 2 ml of the suspension of algal cells passed through the excitation beam in less than one second.

Induction Conditions

The algae were harvested and resuspended in 200 ml of Bishop's growth media contained in a foil-covered flask. The wildtype algae were allowed to dark-adapt for two hours in the light-tight flask. The mutant 8 algae were maintained in their dark-adapted state during harvesting and resuspension. The experimental procedure for preparation of the sample was to pipette two milliliters of the algal suspension into the sample cuvette, block the modulated laser beam from entering the light-tight box containing the sample holder, insert the sample cuvette into the sample holder, insure that the light modulation and trigger signals were correct, and then remove the barrier to allow the modulated

laser beam to enter the light-tight box and strike the sample cuvette. The algal induction periods were timed by a stopwatch, beginning at the instant the laser light first struck the algal sample.

Pulse-height Analysis

The algal sample was harvested, transferred to the sample cuvette, and brought to the steady-state of illumination as described earlier in this chapter. The pulse-height analysis instrumentation and the rotating disc laser modulator were assembled and tested as described in the instrumentation chapter. After the algae had been adapted to the modulated stimulus light, the pulse-height analysis experiments began when the MCA was switched to the "aquire" mode. The progress of the experiment was checked by means of the MCA monitor scope. The data aquisition proceeded automatically while the repetitive modulation of the laser stimulus light caused the algal sample to produce a certain amount of delayed light emission following each stimulus light flash. The experiment ended when the MCA was switched out of the "aquire" mode back to the "display" mode.

The first experiments to be reported are two exper-ments which demonstrate and evaluate the operation of the entire pulse-height analysis system of photon counting. The first experiment recorded scattered stimulus laser light

over a time interval which included the instant of stimulus light extinction. The second experiment of the set recorded the light emitted from the algae over the same time interval. The phototransistor signal from the rotating disc apparatus served as the experimental trigger signal so that a TAC "start" pulse could be generated which would occur some eight microseconds before the instant of stimulus light extinction.

For the first experiment, the 690 nm interference filter was removed from in front of the photomultiplier, the iris was narrowed, and a small portion of the modulated laser light was scattered from the empty sample holder toward the photomultiplier tube housing. Therefore, the only light recorded was the modulated laser stimulus light.

For the second experiment, the 690 nm interference filter was replaced, the iris was opened, and the light emission from the wildtype strain of the Scenedesmus algae was recorded.

Both experiments utilized the twenty microsecond TAC time range. Both experiments utilized the rotating disc apparatus to modulate the laser beam.

The data from the two experiments were normalized to the same maximum value of 100 and plotted together in the same figure. This allowed a direct evaluation of the

magnitude of the delayed light over the pulse-height analysis system noise.

The rotating disc method of stimulus light modulation was used for the pulse-height analysis experiments of the 80 microsecond and 10 microsecond ranges of the TAC. The one microsecond TAC range pulse-height analysis experiments utilized the electro-optical method of laser light modulation. In all of these experiments, the "start" trigger signal for the TAC was delayed only enough to allow the TAC to operate without bias.

The pulse-height instrumentation was also used to measure the first 80 microseconds of delayed light emission from the dark-adapted wildtype and mutant 8 algae under the flow conditions. The dark-adapted algae were illuminated only for a one-second interval as the algal suspension flowed through a quartz viewing tube which was positioned in front of the photomultiplier tube housing. The procedure of these experiments was the same as that of the steady-state conditions experiments with the exception of the flow arrangement for the algal sample.

Prompt Fluorescence/Delayed Fluorescence Ratio

The electro-optical method of modulation of the stimulus laser light was used in another separate group of pulse-height analysis experiments in which the purpose

was to measure the ratio of intensities of an algal sample's delayed light emission at one microsecond after stimulus light extinction. In these experiments, the TAC was operated only on the four microsecond scale. Both the wildtype and the mutant 8 algae were tested under steady-state conditions and under flow conditions. The results of these experiments were combined with the results of the experiments described in the following paragraphs in order to calculate the prompt fluorescence/delayed fluorescence ratios.

A direct measurement of the ratio was not possible during the illumination periods of the algae with the laser light. However, during the first microsecond following the extinction of stimulus light, the level of intensity for delayed light could be measured. The results of the preceeding TAC experiments had already shown that the delayed light intensity changed only a small amount over the first few microseconds following stimulus light extinction. Therefore, the intensity of the delayed light emission in the first microsecond following stimulus light extinction was taken as the level of delayed light emission during illumination. The ratio of the plateau level of prompt fluorescence intensity to the intensity level of the first microsecond of delayed light was designated by the ratio $(FL_{pr} + FL_{dl})/FL_{dl}$, where the subscripts pr and dl designate the prompt fluorescence intensity and the delayed light intensity respectively.

The method of determination of the above ratio was based on the fact that the electro-optical laser light modulators allowed a small amount of light leakage some two to three microseconds after the instant of extinction of the stimulus laser beam by the modulators. As described in the instrumentation chapter, a photodiode and sampling scope were used to record the exact stimulus light modulation waveform. From the data of these recordings, the magnitude of the intensity of the plateau of the stimulus light before the extinction of the laser beam was measured, as was the maximum of the small laser light leakage peak two microseconds following the stimulus light extinction.

After the photodiode-sampling scope experiment was completed, the sampling scope, the signal averager, and the diode were disconnected. The pulse-height analysis system was reassembled and tested as described in the instrumentation chapter. The pulse-height instrumentation was utilized so that the algal light emission could be recorded over the four-microsecond time interval following the instant of stimulus light extinction. The start pulse for the TAC was delayed electronically so as to occur each modulation cycle 0.1 microseconds after the modulator switching point. Since the results of the photodiode experiment were to be related to the results of the TAC experiments, it was imperative that there was no mechanical or electrical

readjustment of the electro-optical laser modulators between the individual experiments.

Two separate experiments utilized the TAC instrumentation in order to measure the four-microsecond time interval following stimulus light extinction. The first experiment was run with an acetone-chlorophyll solution in the sample cuvette. This control sample produced excellent fluorescence at 690 nm, but produced no delayed light emission. The second TAC experiment measured the emission from the wild-type algae or from the mutant 8 strain. The two TAC experiments' data were normalized to 100 at the maximum of the small peak caused by the stimulus light leakage through the electro-optical modulators. Side by side comparison of plots of the normalized data showed the magnitude of the delayed light emission (on the plot of the algal experimental data) relative to the photon counting system noise (on the plot of the acetone-chlorophyll experimental data).

The results chapter describes how the experimental data from the above experiments were used to calculate the intensity of the first microsecond of delayed light emission relative to the intensity of the prompt fluorescence.

Recurrent Multiscaling

The algal sample was prepared and brought to dark-adapted conditions as described previously. The instrumentation for recurrent multiscaling has been described in the

instrumentation chapter. The voltage to the motor was adjusted so that the disc apparatus modulated the stimulus laser light into alternating intervals of five milliseconds of light and darkness at the algal sample holder site.

The experimental procedure was to first adjust the laser and the rotating disc apparatus for proper stimulus light modulation. The modulated light beam was then blocked at the point of entry into the light-tight box containing the sample cuvette. The cuvette was then filled with the suspension of dark-adapted algae and placed into the sample holder. The purpose of the experiment was to make four one-minute MCA recordings by repetitive multiscaling in order to record the time sequence of the decay of intensity of delayed light emission from an individual algal sample. The four recording periods were spaced through the first eleven minutes of the algal light induction period.

The first recording period began as soon as the light barrier was removed, allowing the modulated laser beam to strike the algal sample. After sixty seconds, the MCA was switched out of the aquire position, the selection of the second 256-channel group of the MCA was made by turning the memory-group selection switch, and when the next recording period was to begin, the MCA was switched back to aquire for the next 60-second recording period. The second, third, and fourth recording periods were initiated when the algal

sampl

for 1

the

Afte

of t

repl

reac

rep

exp

ing

per

mM/

exp

wer

Cha

sio

in

wil

des

app

alt

sample had been exposed to the modulated laser beam for 120 seconds, 300 seconds, and 600 seconds. Both the wildtype and the mutant 8 algal strains were tested. After the four recording periods, the four memory groups of the MCA were read out via the Teletype, the algal sample replaced by a fresh dark-adapted sample, and the apparatus readied for another experiment.

Four experiments utilizing the wildtype algae are reported in this recurrent multiscaling section. Each experiment consisted of four one-minute multiscaling recordings of the delayed light emission. Each experiment was performed with a different stimulus light intensity: 0.11 mW/cm^2, 2.25 mW/cm^2, 22.5 mW/cm^2, and 59 mW/cm^2. One experiment is reported here in which the mutant 8 algae were utilized.

Single Sweep Multiscaling

The purpose of these experiments was to record the changes in the first 60 microseconds of delayed light emission during induction periods of 820 seconds. The changes in the prompt fluorescence were also recorded for both the wildtype and the mutant 8 algae.

The instrumentation for single sweep multiscaling was described in the instrumentation chapter. The rotating disc apparatus was used to modulate the stimulus light into alternating intervals of five milliseconds of stimulus laser

light at the algal sample holder site, followed by five milliseconds of darkness at the sample site.

The algal sample was prepared, brought to dark-adapted conditions, transferred to the sample cuvette, and inserted into the sample holder while the modulated laser beam was blocked at the site of entry of the beam into the box surrounding the sample holder. The MCA was switched to "aquire" in order to start the single sweep multiscaling experiments. The stimulus light was introduced to the sample site several seconds after the start of the MCA.

The first experiment recorded the change in the wildtype prompt fluorescence during the induction period. The prompt fluorescence was recorded by adjusting the delay of the gate pulse generator so that the 60 microsecond gate interval occurred during illumination of the algal sample. For this experiment, the iris in front of the photomultiplier tube had to be narrowed so that the high pulse count rate would not overload the MCA input circuit. The second experiment was a repeat of the first, except that the mutant 8 algae were used instead of the wildtype algae.

The third experiment was a recording of the first 60 microseconds of delayed light emission from the wildtype algae during the induction period. The gate pulse delay was adjusted so as to occur less than five microseconds after the instant of stimulus light extinction at the sample site.

The fourth experiment was a recording of the first 60 microseconds of delayed light emission from mutant 8 algae during the 820 second induction period.

The fifth, sixth, and seventh experiments were repeats of the fourth experiment utilizing different stimulus light intensities. In these last three experiments, the percentage decrease in stimulus light intensity was exactly compensated for by opening the iris to admit more delayed light to the photomultiplier tube. Thus, the count rate was about the same during each of the last three experiments.

Data Handling

At the completion of each experiment, the data of the experiment had to be recovered from the MCA memory bank. The output device was a Model 33 KSR Teletype machine which was interfaced to the MCA by an electronic Teletype driver module. During the read-out process, the Teletype machine simultaneously printed the data with the printer mechanism and punched paper tape with the paper tape punch mechanism of the machine. The punched paper tape was later read onto magnetic tape and the data of the magnetic tape was processed, printed, and plotted on-line by the Michigan State University Control Data Corporation 3600 computer. All plots of experimental data of this thesis are plots drawn by the computer.

RESULTS

Pulse Height Analysis

Evaluation of Photon Counting System

Figure 4 is a plot of the data from the two demonstration experiments which were run with the 20 microsecond TAC scale in order to demonstrate the operation of the pulse-height analysis system of photon counting. The time interval covered by the plot extends from eight microseconds preceeding the instant of light extinction to some 12 microseconds following light extinction. The curve on the plot which leads to the scattered points along the bottom of the figure is the curve representing the data from an experiment in which a small portion of the modulated laser beam was scattered from the sample holder toward the photomultiplier tube. As was described in the methods chapter, the 690 nm interference filter was removed from its position in front of the photomultiplier tube for the duration of the scattered light experiment.

The light emission from the wildtype strain of Scenedesmus algae was recorded in the second experiment.

The normalized data from this experiment forms the curve which ends in the rather horizontal line across the center of the right side of Figure 4.

Both experiments utilized the rotating disc apparatus to modulate the laser beam. An adjustment of the rotating disc apparatus had to be made between the two experiments and the adjustment affected the phototransistor trigger signal, resulting in the lack of congruence of the left third of the scattered light curve with the left third of the algal emission curve.

A careful examination of the two curves of Figure 4 allows evaluation of the operation of the pulse-height analysis system and evaluation of the magnitude of the photon counting system noise. From Figure 4 one can determine that the on:off contrast ratio was about 10,000:1 in the scattered light experiment. From the curve representing the wildtype algal light emission, one can determine that the ratio of the intensity of prompt fluorescence to the intensity of the first microsecond of delayed light emission is greater than 1000:10 (100:1) but less than 1000:5 (200:1). One can also estimate the relative magnitude of the delayed light emission signal as compared to the electronic system noise which was recorded in the scattered light curve over the same time interval as that of the delayed light. An inspection of Figure 4 shows that the magnitude of the first

microsecond of delayed light signal was about 5.0 on the ordinate scale. Division of 5.0 by 0.12 gives a ratio of 41:1 as the ratio of the signal amplitude over the noise amplitude. In conclusion, the results of the demonstration experiments accomplished the purpose of the experiments: to allow evaluation of the photon counting system operation and to allow evaluation of the magnitude of the signal to that of the system noise.

The TAC experiments reported in the following figures, Figures 5 to 10, recorded the delayed light emission from the algae as a function of time after the 488 nm laser stimulus light had been extinguished. One must remember that the origin of the time axis in these figures was located at the beginning of the light extinction.

Figure 5 is a plot of the normalized data from a TAC experiment recording the first 80 microseconds of delayed light emission from the mutant 8 strain of algae. The time scale of the figure begins at a point some four microseconds before light extinction and the curve of the figure is a recording of delayed light emission which occurred after light extinction, except for the first eight dots on the left end of the curve. From the figure, one can see that the emission intensity decreased by a factor of two in the first 80 microseconds after the extinction of the stimulus light beam.

Figure 6 is a plot of the normalized data from an experiment which recorded the first 80 microseconds of delayed light emission from the wildtype strain of the Scenedesmus algae. Note that the decay of the delayed light emission from the wildtype algae resembles the decay of the light emission from the mutant 8 strain.

The first eight microseconds of the mutant 8 delayed light emission curve was recorded at higher resolution in TAC experiments with the 8-microsecond range of the TAC. The time axis of Figure 7 begins at the instant of stimulus light extinction. Since the light extinction took 0.25 microseconds to complete, the TAC recording of Figure 7 shows a small component of the prompt fluorescence in the first twenty dots of the curve. The prompt fluorescence from the algae results from their exposure to the final nanoseconds of the stimulus light extinction.

Figure 8 shows the decay curve of the delayed light emission from the wildtype strain of the algae for the same ten microseconds following stimulus light extinction. In the experiment which recorded this set of data, the start pulse which triggered the TAC was synchronized so as to precede the instant of stimulus light extinction. For this reason the final nanoseconds of stimulus light extinction produced prompt fluorescence from the algae and this fluorescence was recorded in the first 20 or 30 channels.

An experiment utilizing the 0.8 microsecond TAC range recorded the data which are plotted in Figure 9. For this recording of the delayed light from the mutant 8 algae, the origin of the time axis was located again at a point before the stimulus light extinction was complete and this fact is shown in the figure by the rapidly decaying prompt fluorescence component of the first 20 points of the curve.

Figure 10 is a TAC recording of the first 1.0 microseconds of delayed light from the wildtype strain. In this figure, the trailing edge of the prompt fluorescence can be seen in the first ten dots of the curve.

Figure 9 and Figure 10 both show that the rapidly decaying prompt fluorescence curve rather abruptly intersects the delayed light emission curve of mutant 8 algae or wildtype algae. There is no evidence of an exponential decay between the end of the prompt fluorescence curve and the start of the observable delayed light emission curve. Nor is there indication that the delayed light emission begins at the instant of light extinction. Instead, the delayed light emission curve intersects the decaying prompt fluorescence curve at virtually a right angle when the curves are plotted on a one-microsecond time scale. The significance of these observations will be explained in the discussion chapter.

There were two pulse-height analysis experiments that

Figure 4. A plot of the normalized data of the two demonstration TAC experiments which compares the magnitudes of the wildtype algal delayed light emission signal (upper curve) with the system noise (lower curve).

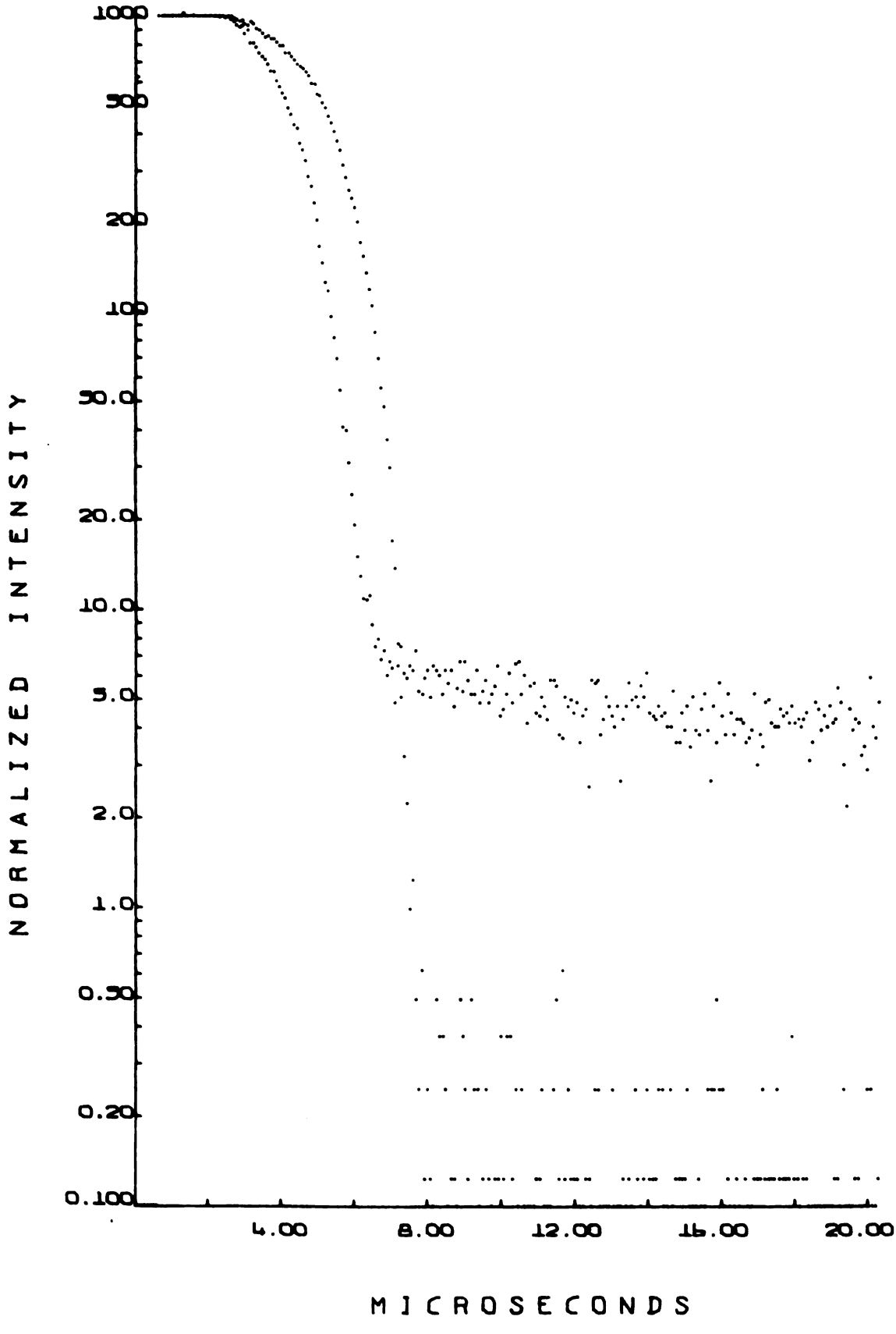
NORMALIZED INTENSITY
100
50
20
10
5.0
2.0
1.0
0.50
0.20
0.100
4.00
8.00
12.00
16.00
20.00
MICROSECONDS

Figure 5. Decay curve of the first 80 microseconds of delayed light emission from the mutant 8 algae.

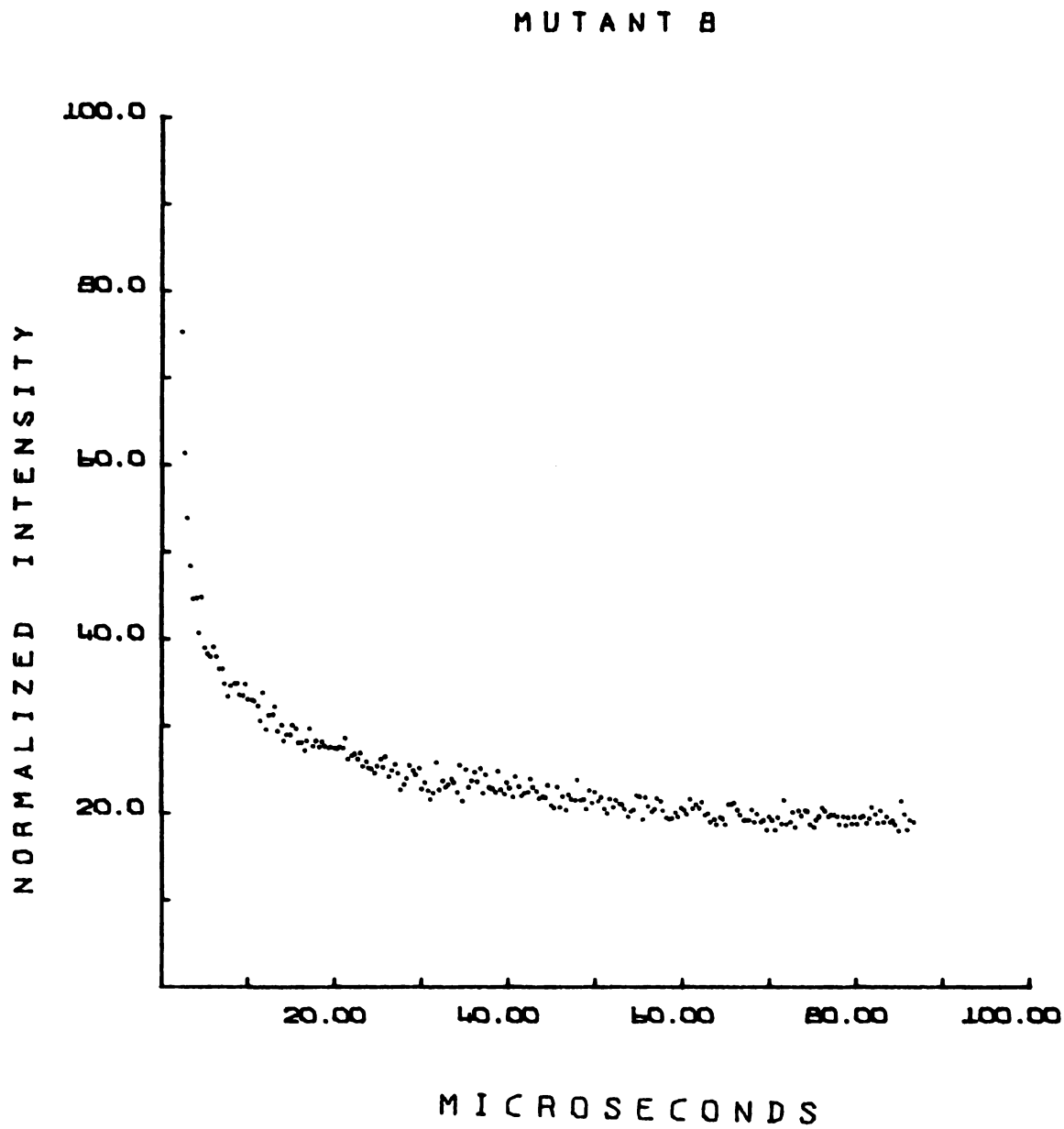
MUTANT 8
100.0
80.0
60.0
40.0
20.0
NORMALIZED INTENSITY
20.00
40.00
60.00
80.00
100.00
MICROSECONDS

Figure 6. Decay curve of the first 80 microseconds of delayed light emission from the wildtype algae.

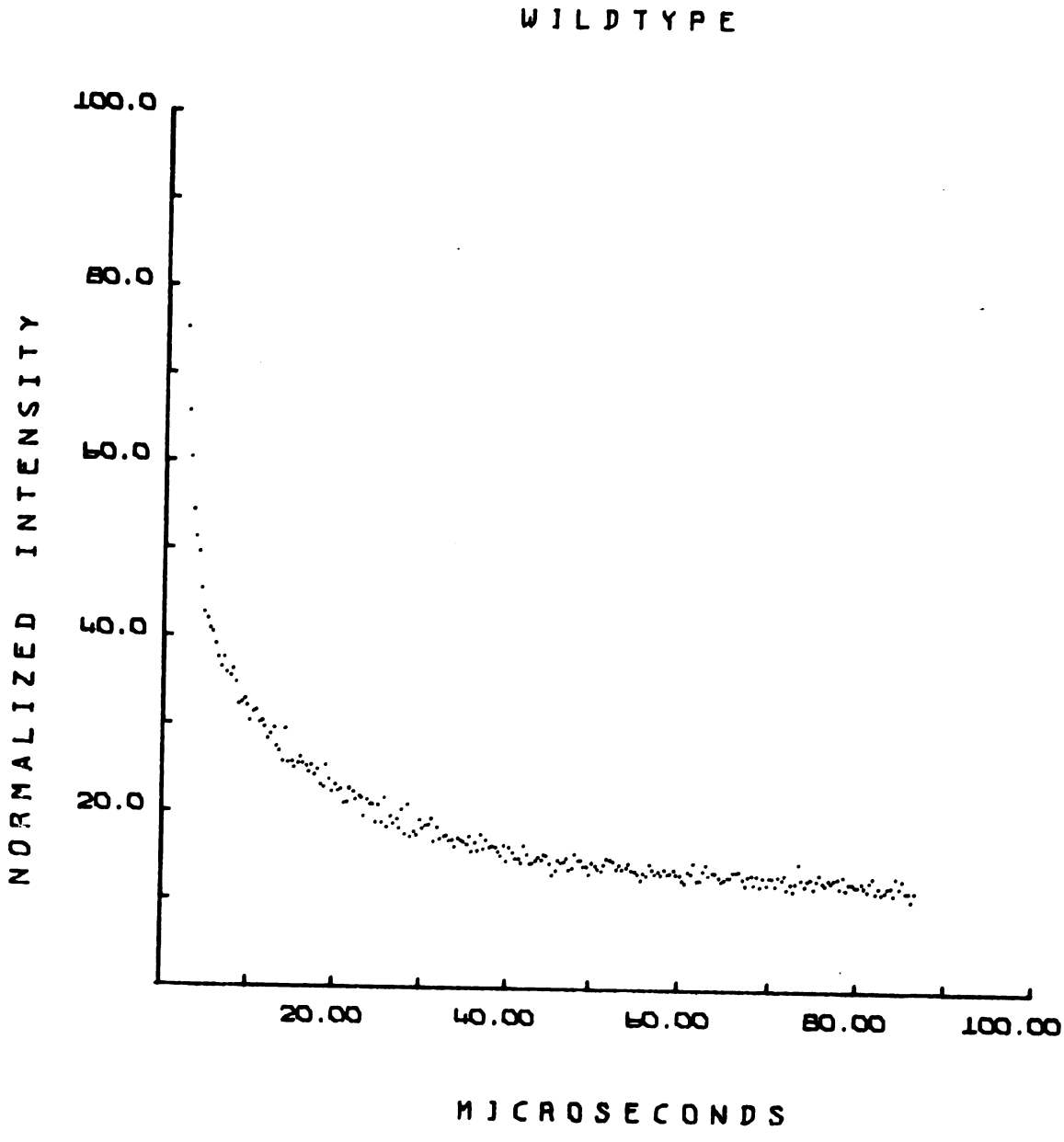
WILDTYPE
NORMALIZED INTENSITY
100.0
80.0
50.0
40.0
20.0
20.00
40.00
60.00
80.00
100.00
MICROSECONDS

Figure 7. Decay curve of the first eight microseconds of delayed light emission from the mutant 8 algae.

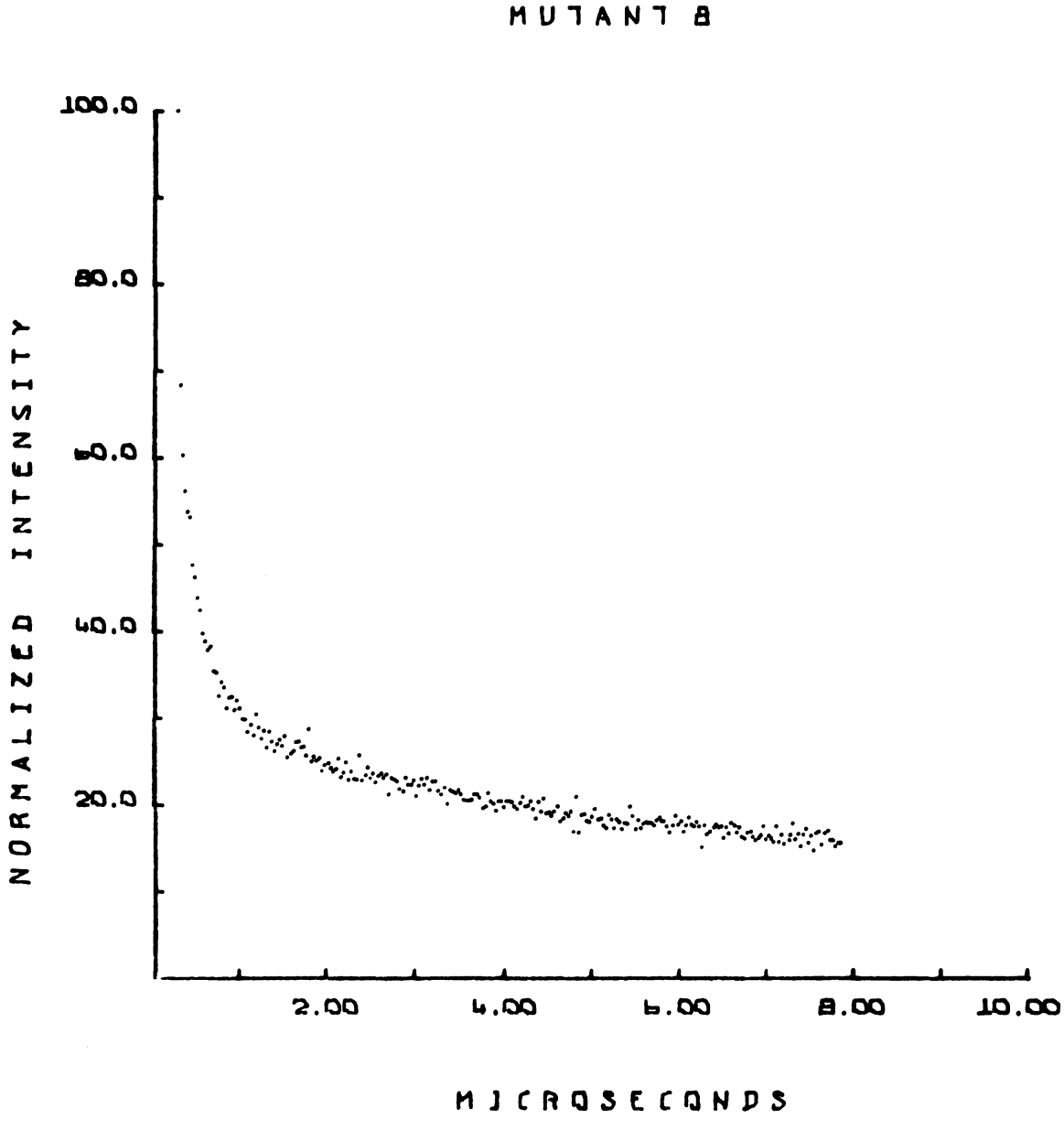
MUTANT B
100.0
80.0
60.0
40.0
20.0
NORMALIZED INTENSITY
2.00
4.00
6.00
8.00
10.00
MICROSECONDS

Figure 8. Decay curve of the first ten microseconds of delayed light emission from the wildtype algae.

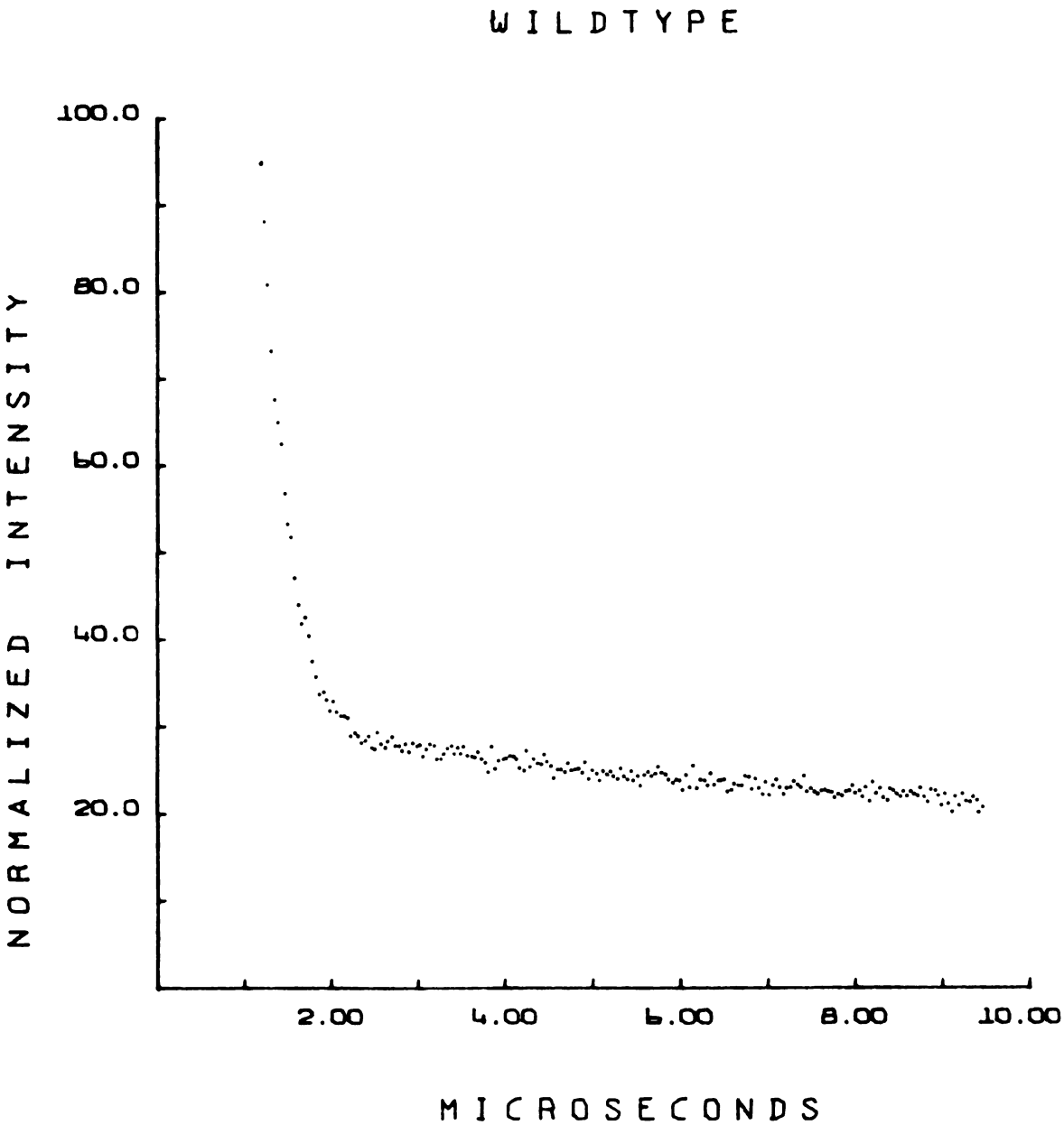
WILDTYPE
100.0
80.0
50.0
40.0
20.0
NORMALIZED INTENSITY
2.00
4.00
6.00
8.00
10.00
MICROSECONDS

Figure 9. Decay curve of the first 0.8 microseconds of delayed light emission from the mutant 8 algae.

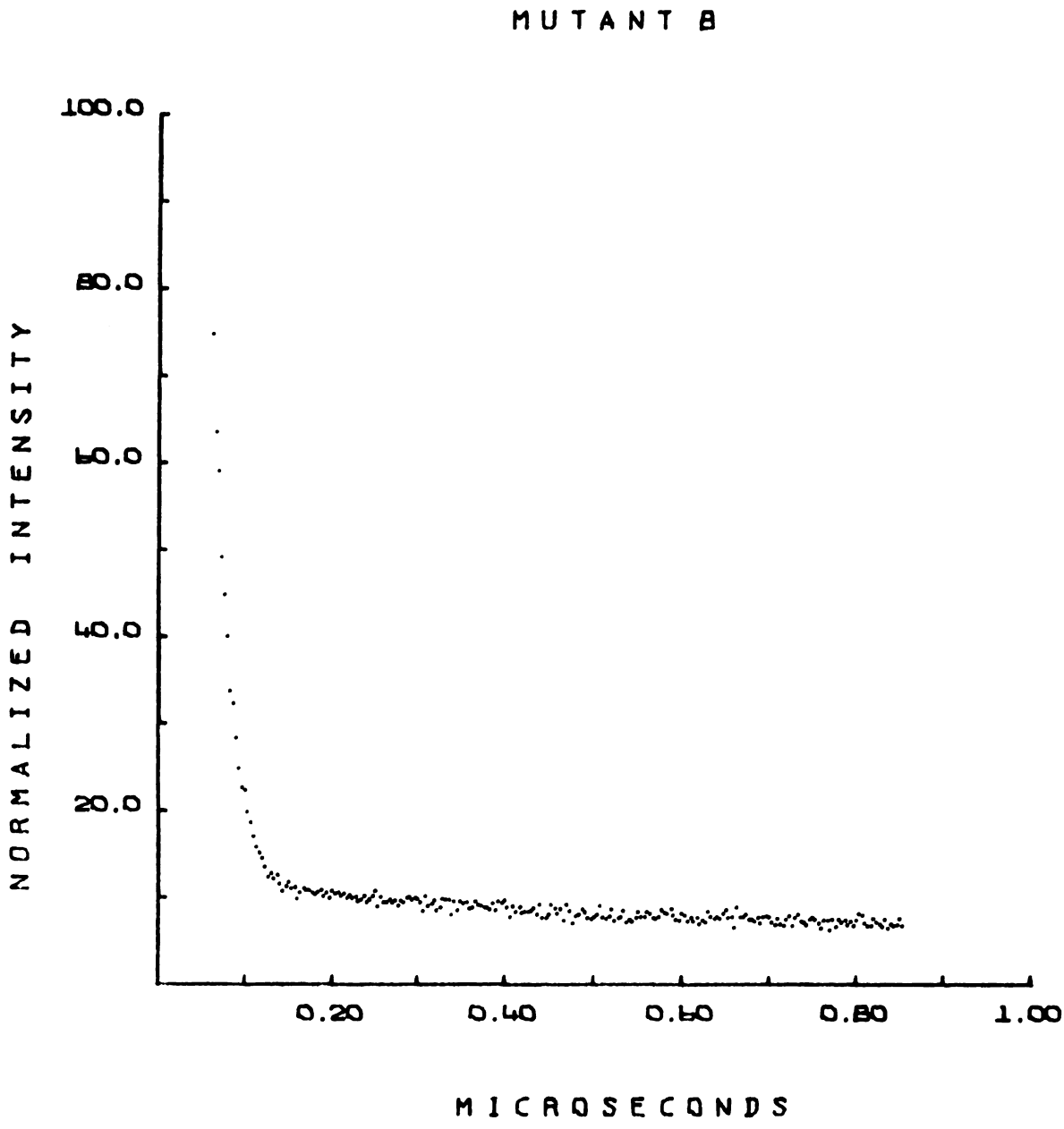
MUTANT B
100.0
80.0
60.0
40.0
20.0
NORMALIZED INTENSITY
0.20
0.40
0.60
0.80
1.00
MICROSECONDS

Figure 10. Decay curve of the first microsecond of delayed light emission from the wildtype algae.

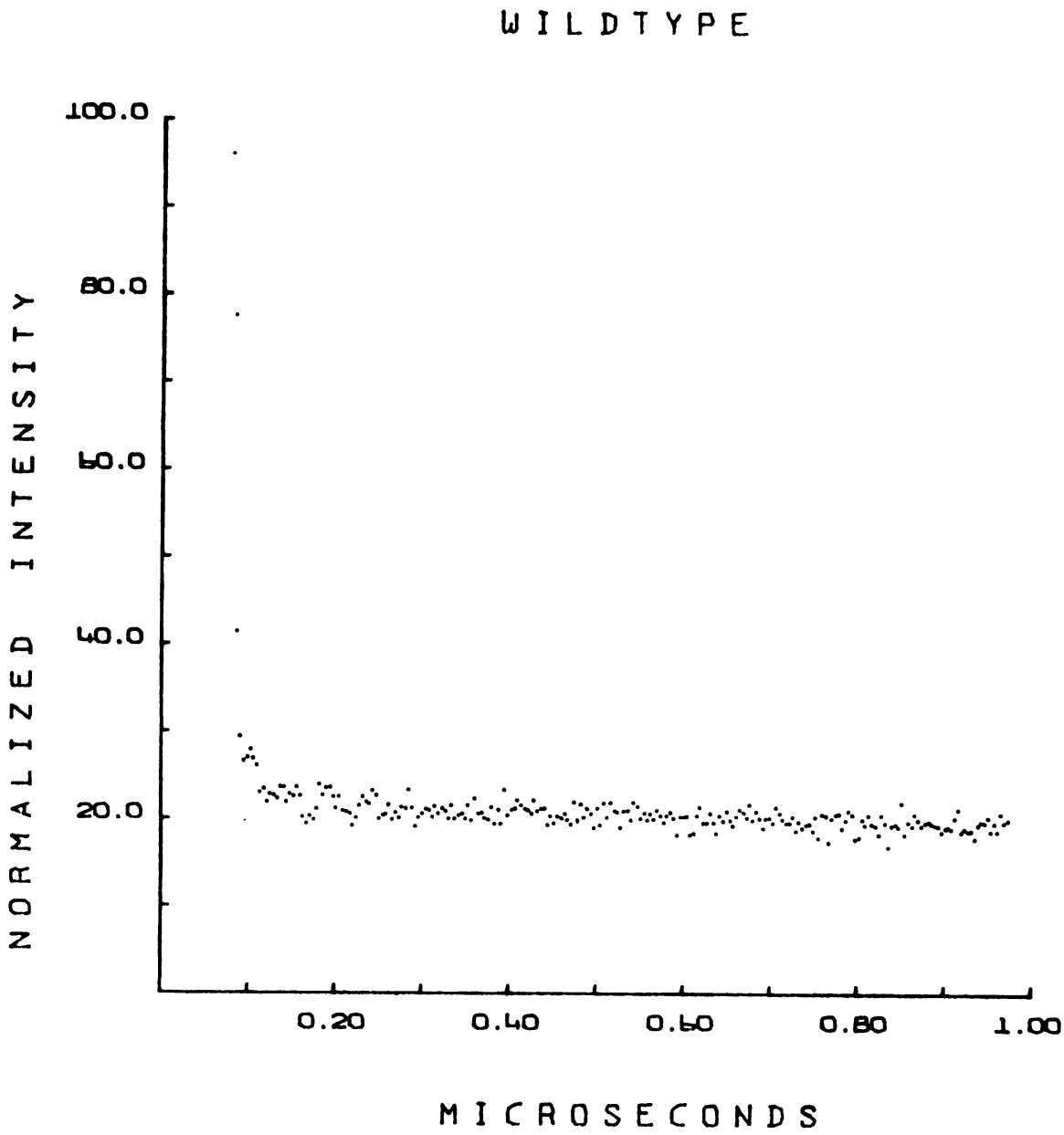
WILDTYPE
100.0
80.0
60.0
40.0
20.0
NORMALIZED INTENSITY
0.20
0.40
0.60
0.80
1.00
MICROSECONDS

Figure 11. Comparison of 80-microsecond TAC flow experiments' data from dark-adapted wildtype algae (upper curve) and from dark-adapted mutant 8 algae (lower curve).

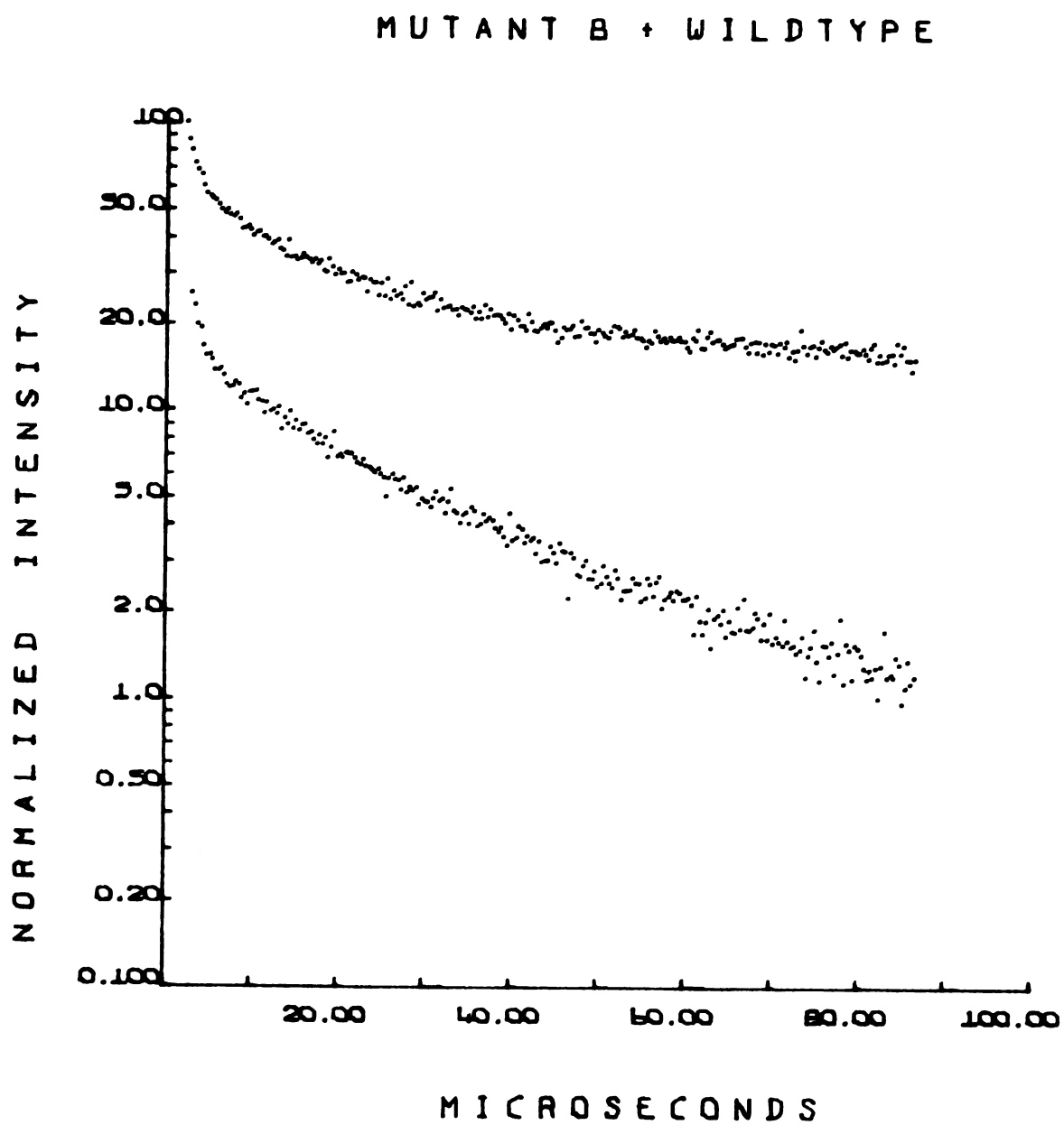
MUTANT B + WILDTYPE
NORMALIZED INTENSITY
100.
50.0
20.0
10.0
5.0
2.0
1.0
0.50
0.20
0.100
20.00
40.00
60.00
80.00
100.00
MICROSECONDS

measured the first 80 microseconds of delayed light emission from dark-adapted algae during flow conditions. The normalized data from the two experiments are plotted together in one plot, Figure 11. The figure was plotted with a logarithmic ordinate axis in order to allow direct comparison of the decay of delayed light emission from the dark-adapted wildtype algae and from the dark-adapted mutant 8 algae under the flow conditions. The figure shows that the slope of the wildtype data is smaller than the mutant 8 data, indicating that the kinetics of decay of the first seconds of delayed light is different in the two strains of algae during flow conditions.

Prompt Fluorescence/Delayed Fluorescence Ratios

The results of a typical set of experiments for the determination of the prompt fluorescence/delayed fluorescence ratio are presented in Figures 12 through 15. Figure 12 is a plot of the data from the photodiode-sampling scope experiment in which the waveform of the stimulus light modulation was recorded. Figure 13 is a plot of a subsequent pulse-height analysis experiment which recorded the 690 nm light emission from a chlorophyll-acetone solution. Figure 14 is a plot of the wildtype algal emission at 690 nm, while Figure 15 is a plot of the emission at 690 nm from the mutant 8 algal sample. As explained in the procedure chapter, no electrical or mechanical adjustments of the light modulation

Figure 12. Time course of the extinction of laser stimulus light by the electro-optical laser modulators.

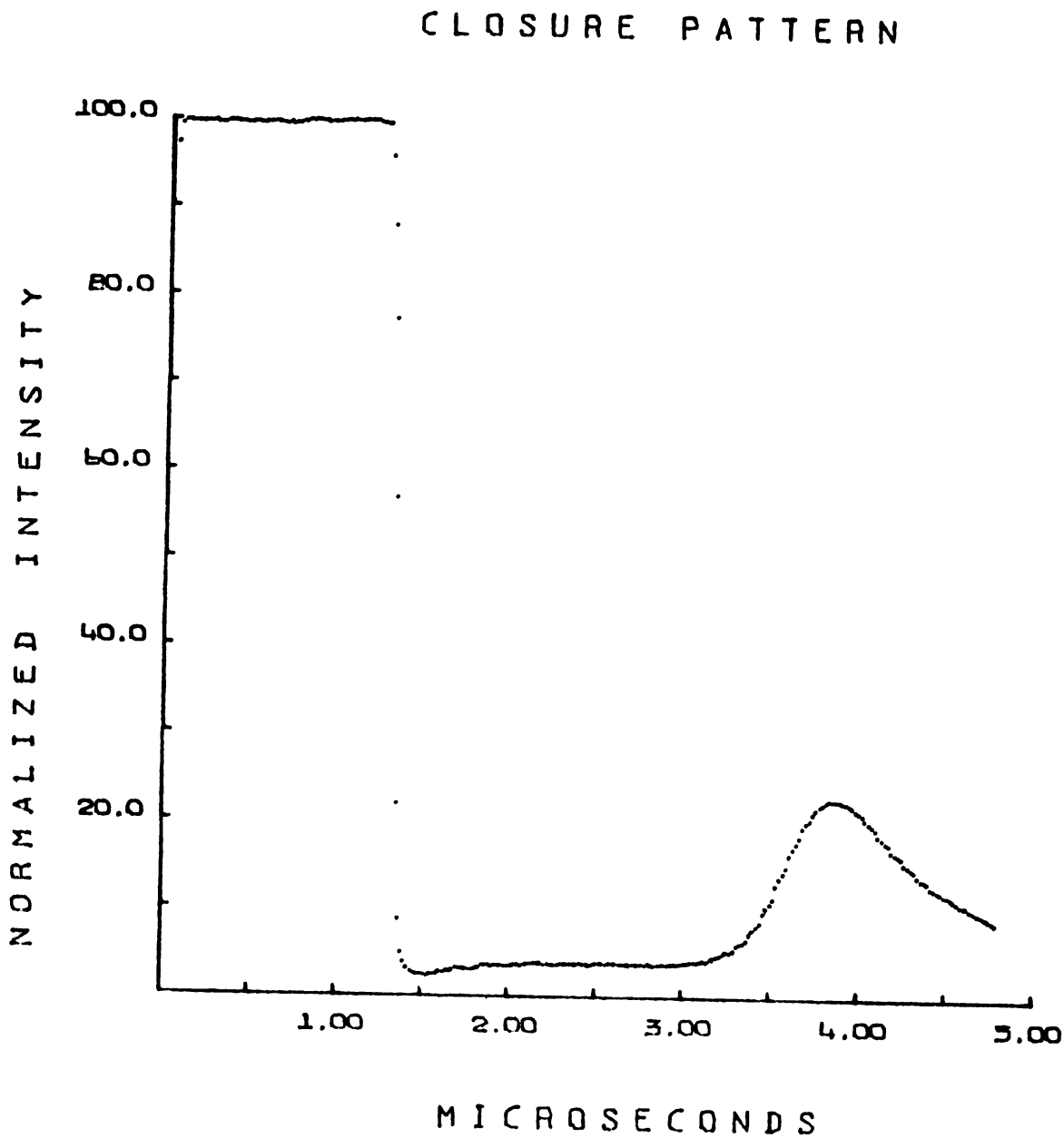
CLOSURE PATTERN
100.0
80.0
60.0
40.0
20.0
NORMALIZED INTENSITY
1.00
2.00
3.00
4.00
5.00
MICROSECONDS

Figure 13. First four microseconds of fluorescence emission from a solution of algal chlorophyll in acetone.

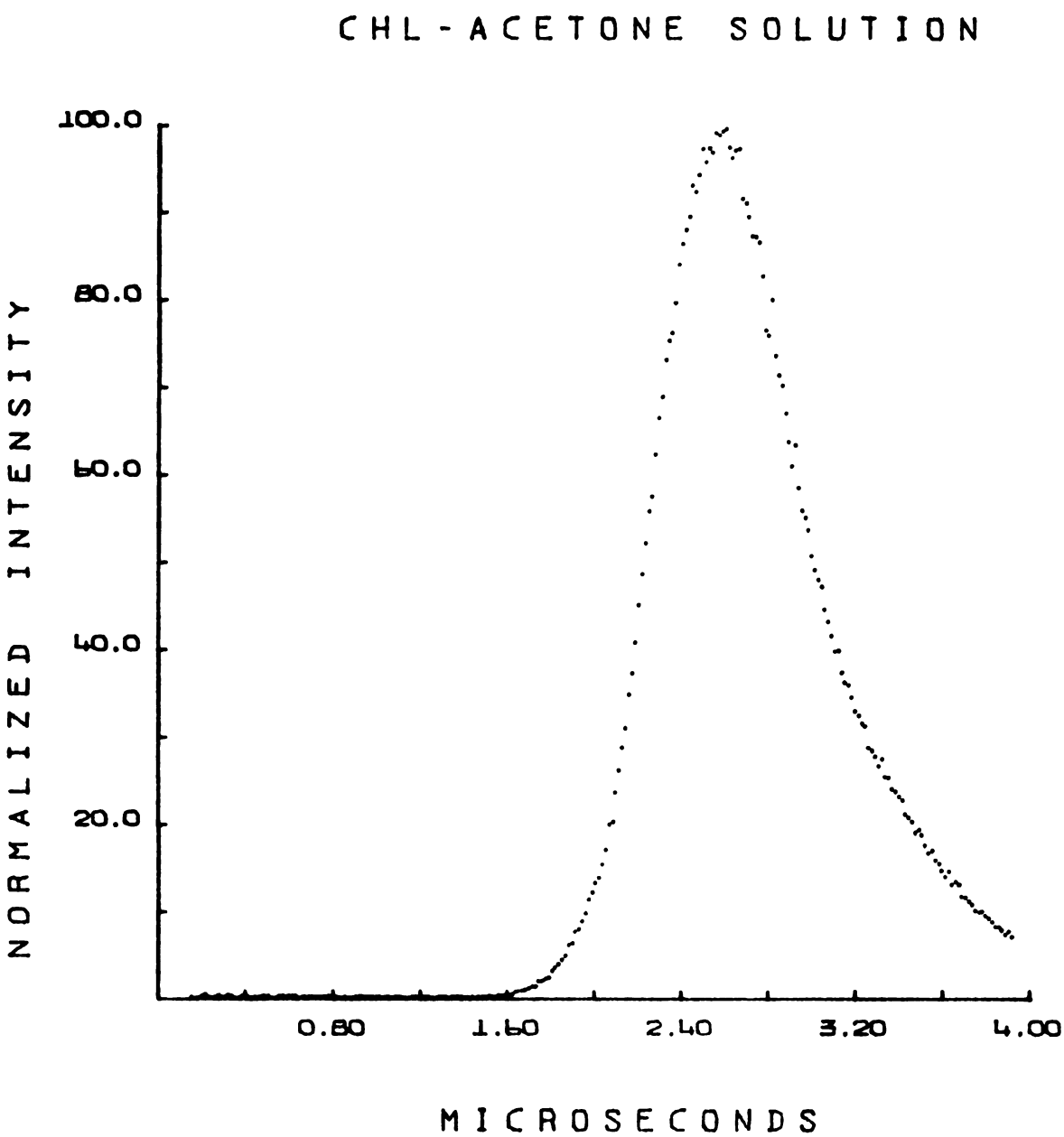
CHL-ACETONE SOLUTION
NORMALIZED INTENSITY
100.0
80.0
50.0
20.0
0.80
1.60
2.40
3.20
4.00
MICROSECONDS

Figure 14. First four microseconds of light emission from a suspension of the wildtype algae.

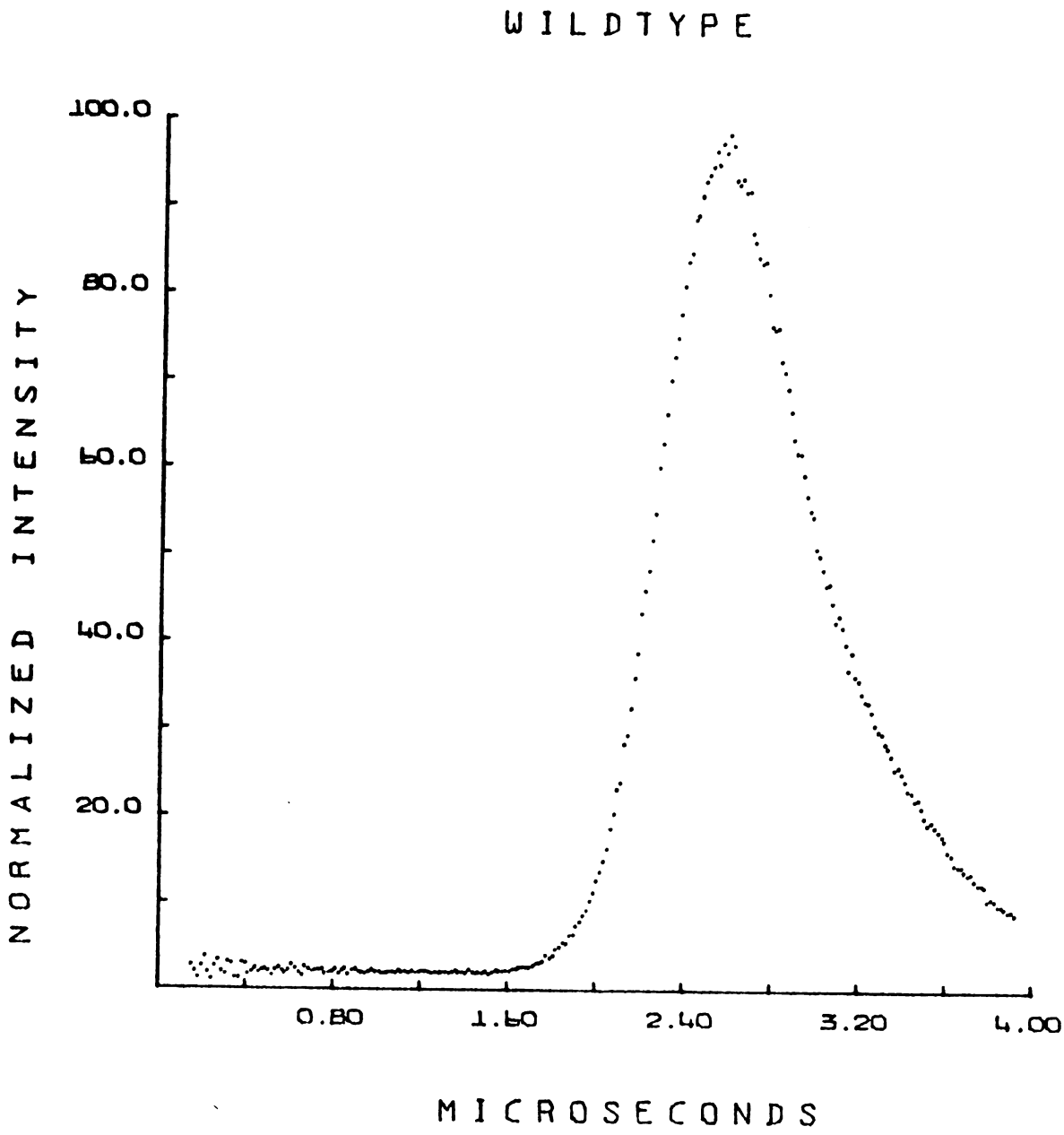
WILDTYPE
100.0
80.0
60.0
40.0
20.0
NORMALIZED INTENSITY
0.80
1.60
2.40
3.20
4.00
MICROSECONDS

Figure 15. First four microseconds of light emission from a suspension of the mutant 8 algae.

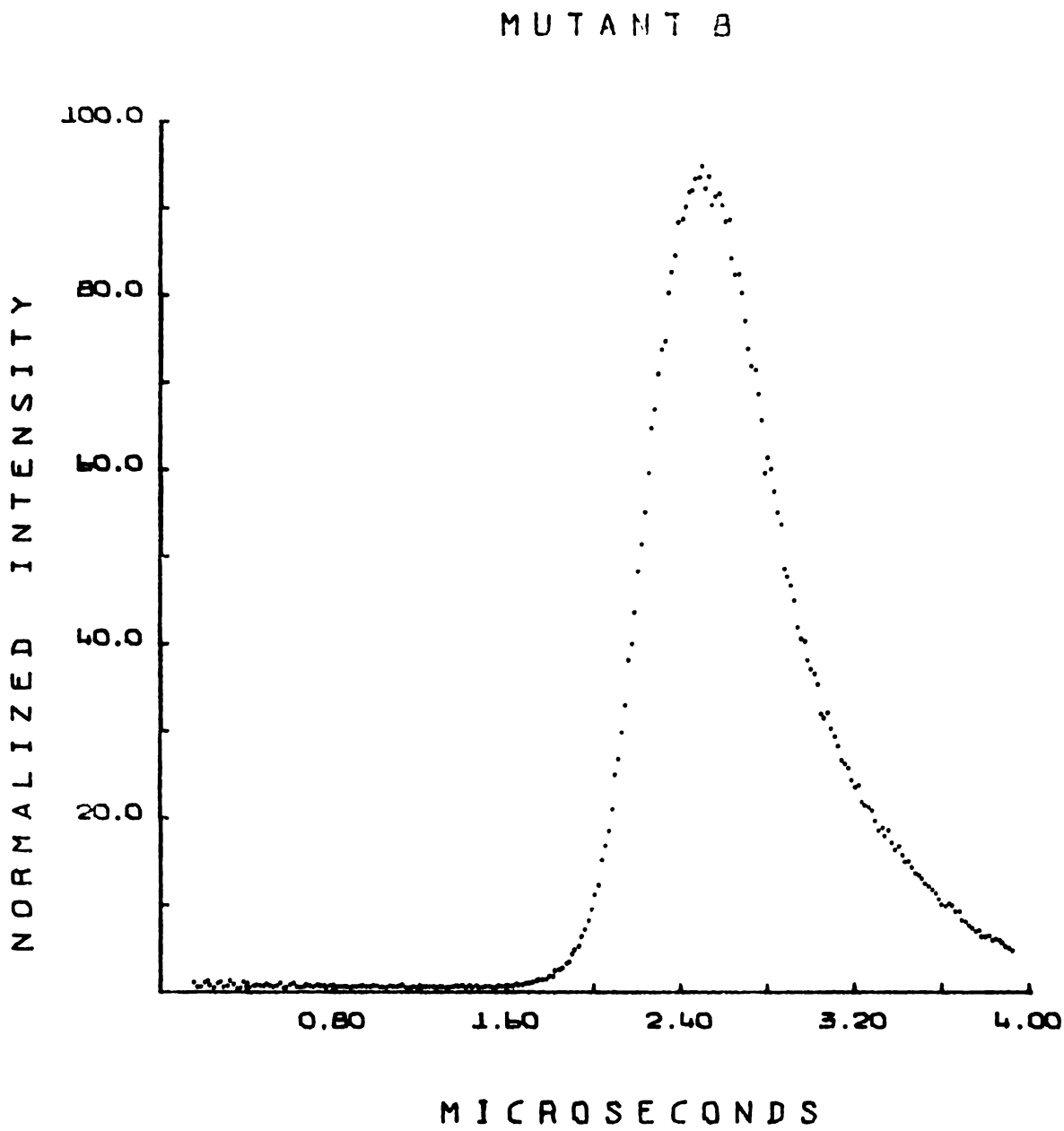
MUTANT B
100.0
80.0
60.0
40.0
20.0
NORMALIZED INTENSITY
0.80
1.60
2.40
3.20
4.00
MICROSECONDS

apparatus were made between the individual experiments of a particular set of experiments. The following paragraphs discuss the calculations necessary to determine the prompt fluorescence/delayed fluorescence ratio from a typical set of experiments. The discussion outlines the assumptions by which the calculation can be simplified to the product of two ratios.

Calculations of Fluorescence/Delayed Light Ratios

The purpose of the following calculation is to analyze the factors affecting the ratio of prompt fluorescence to delayed fluorescence during the steady state illumination. The two components of the ratio can not be measured directly, but the ratio can be calculated very simply after consideration of the magnitudes of the various emissions which are measured during the TAC experiments with the chlorophyll solution and with the algae.

Below is a list of parameter definitions used in the calculation.

A: Time region of the plateau of steady state illumination before laser light extinction.

B: Time of occurrence of the maximum of the light leakage peak.

C: Time interval along the first measurable segment of the delayed light emission curve in the TAC experiments, i.e., about 0.2 microseconds following the instant of laser light extinction.

FL_A: Prompt fluorescence intensity at time A.

FL_B: Prompt fluorescence intensity at time B.

FL_C: Prompt fluorescence intensity at time C.

DL_A: Delayed light intensity at time A.

DL_B: Delayed light intensity at time B.

DL_C: Delayed light intensity at time C.

The ratio of FL_B/FL_C was evaluated from the data of the chlorophyll-acetone solution TAC experiment. Since this ratio was always found to be greater than 2500:1, the value of FL_C was neglected in the following calculations. If the FL_C value was small enough to be neglected, the DL_C delayed light component could also be neglected since the DL_C value would be expected to be some two orders of magnitude smaller than FL_C. Therefore, at time B, the observed algal emission could be attributed to three components,

$$FL_B + DL_B + DL_A$$

and the emission intensity at time C could be attributed only to the DL_A term.

The ratio of algal emission intensity at time B, E_B, to algal emission intensity at time C, E_C, could then be expressed as E_B/E_C and evaluated by the relation

$$(FL_B + DL_A + DL_B)/DL_A = E_B/E_C \ .$$

Expansion of the left side of the above equation gives

$$\frac{FL_B}{DL_A} + \frac{DL_A}{DL_A} + \frac{DL_B}{DL_A} = \frac{E_B}{E_C} \ .$$

Rearranging the above equation gives

$$\frac{FL_B}{DL_A} = \frac{E_B}{E_C} - \left(1 + \frac{FL_B}{FL_A} \right),$$

where the ratio of DL_B/DL_A was set equal to the ratio FL_B/FL_A, assuming that the delayed light emission was proportional to the prompt fluorescence under the steady state conditions of the TAC experiments.

The value of FL_B was related to the value of FL_A by the assumption that the fluorescence was proportional to the excitation light intensity at times B and A, as measured by the photodiode-sampling scope experiment,

$$\frac{FL_B}{FL_A} = \frac{I_B}{I_A}.$$

Solving the above relation for FL_B,

$$FL_B = FL_A \left(I_B / I_A \right).$$

Substituting this value of FL_B into the equation for FL_B/DL_A, one obtains

$$\left(\frac{I_B}{I_A} \right)\left(\frac{FL_A}{1} \right)\left(\frac{1}{DL} \right) = \frac{E_B}{E_C} - \left(1 + \frac{FL_B}{FL_A} \right).$$

Multipling both sides of the equation by (I_A/I_B) leaves the desired ratio, FL_A/DL_A, on the left side of the equation

$$\frac{FL_A}{DL_A} = \left(\frac{I_A}{I_B}\right)\left[\frac{E_B}{E_C} - \left(1 + \frac{FL_B}{FL_A}\right)\right].$$

Substitution of the proper values into the right side of above formula allowed evaluation of the ratio FL_A/DL_A. Note that less than a three percent error results if the formula is simplified to the following formula, which may be readily evaluated:

$$\frac{FL_A}{DL_A} = \left(\frac{I_A}{I_B}\right)\left(\frac{E_B}{E_C}\right).$$

The value of the ratio I_A/I_B was determined directly by the photodiode experiment, while the emission ratio E_B/E_C was evaluated from the four-microsecond TAC experiment with the algal sample.

The values I_A and I_B were determined by inspection of the MCA Teletype listing of the data of the photodiode-sampling scope experiment. First, the maximum amplitude of the small peak, I_B, was determined. Then, ten to fifteen points of the plateau region of the curve were averaged in order to find the average amplitude, I_A, of the curve in region A. There was usually some baseline drift in these experiments, and this was detected by noting the amplitude of the curve in region C where there should have been no light striking the photodiode. The average of the baseline

drift amplitude was calculated, and this value was subtracted from both the I_A and the I_B value.

The values of E_B and E_C were determined from the MCA data of the four-microsecond TAC experiments with the algae. After each TAC experiment with the algae, the experiment was repeated (with identical instrument settings) with the sample of the chlorophyll-acetone solution. This solution gave strong prompt fluorescence at 690 nm but no delayed light emission. The data from these chlorophyll-acetone experiments served as the controls for the algal experiments. The data of the two experiments were normalized to the same value at the small peak maximum. Then, the amount of noise recorded in region C in the chlorophyll-acetone experiment was subtracted from the data of the algal experiments. The corrected algal curves were the ones used in the determination of the relative E_B and E_C values.

Table 2 shows the results of the ratio calculations for algae during steady state conditions. The ratios for all three algal strains are listed in the table. The table shows that the ratio for the wildtype algae was in the vicinity of 175/1 when the algae were illuminated with 22 mW/cm^2 modulated laser light. The ratio for the mutant 8 strain varied from a value of 160/1 to 1800/1. As will be seen in later experiments in this thesis, the variation in the ratios of the mutant 8 algae resulted from large changes

Table 2. Results of TAC experiments measuring light emission ratios (E_B/E_C), and intensity ratios (I_A/I_B), together with the calculated ratios of the intensity of fluorescence to that of delayed light (FL_A/DL_A).

Algal Strain	E_B/E_C	I_A/I_B	FL_A/DL_A	Light Intensity
	43.2/1	3.76/1	162/1	20 mW/cm^2
	62.1/1	3.28/1	200/1	20 mW/cm^2
	42.5/1	4.16/1	177/1	20 mW/cm^2
	39.5/1	4.40/1	174/1	20 mW/cm^2
	38.6/1	4.52/1	174/1	20 mW/cm^2
Wildtype	40.8/1	4.73/1	193/1	20 mW/cm^2
	27.6/1	8.01/1	221/1	0.01 mW/cm^2
	41.2/1	5.06/1	209/1	0.02 mW/cm^2
	35.2/1	5.06/1	178/1	0.05 mW/cm^2
	37.3/1	5.06/1	188/1	1.30 mW/cm^2
	85.2/1	4.45/1	380/1	20 mW/cm^2
	37.3/1	4.45/1	166/1	20 mW/cm^2*
	63.8/1	8.20/1	523/1	20 mW/cm^2
	128.0/1	3.35/1	429/1	20 mW/cm^2
	287.0/1	3.80/1	1090/1	20 mW/cm^2
Mutant 8	277.0/1	3.80/1	1055/1	20 mW/cm^2
	169.0/1	4.50/1	767/1	20 mW/cm^2
	341.0/1	4.73/1	1612/1	20 mW/cm^2
	74.0/1	14.70/1	1103/1	20 mW/cm^2
	257.0/1	6.88/1	1766/1	20 mW/cm^2
	260.0/1	6.88/1	1790/1	20 mW/cm^2
Mutant 11	2320.0/1	4.73/1	10980/1	20 mW/cm^2

*5 minutes preillumination.

in the intensity of delayed light emission for the mutant 8 algae, and not from large changes in the intensity of the prompt fluorescence, i.e., the ratio variation was due to changes of the denominator of the FL_A/DL_A ratio, and not from change in the numerator of the ratio.

The notes on the side of the table indicate that the ratio was highly dependent upon the preillumination time for the mutant 8 algae. The explanation for this preillumination dependency will also be investigated in the next sections.

Note also from Table 2 that the ratio of the wildtype algae depended somewhat on the intensity of the laser light stimulus. This can be seen in the final four listed experiments for the wildtype algae in Table 2.

The steady state experiments were followed by experiments under flow conditions in order to determine the prompt fluorescence/delayed fluorescence ratio for dark-adapted algae during the first second of illumination. Table 3 presents the results of these experiments, together with the calculated ratios. One can immediately notice that the ratios calculated for these experiments with the algae in the flow conditions are different from the ratios calculated for the experiments with the algae in the steady state conditions of illumination. For the wildtype strain, the ratios reported in Table 3 are only slightly different from

Table 3. Results of flow TAC experiments measuring light emission ratios (E_B/E_C), and intensity ratios (I_A/I_B), together with the calculated ratios of the intensity of fluorescence to that of the delayed light (FL_A/DL_A).

Algal Strain	E_B/E_C	I_A/I_B	FL_A/DL_A	Light Intensity
	22.22/1	7.04/1	156.5/1	20 mW/cm^2
Wildtype	34.70/1	4.24/1	147.0/1	20 mW/cm^2
	25.00/1	4.24/1	106.0/1	20 mW/cm^2
Mutant 8	18.80/1	4.24/1	79.7/1	20 mW/cm^2

the 175/1 ratio measured during steady state conditions. For the mutant 8 strain, the ratio was 80/1 for the algae in the flow conditions, whereas it varied from 160/1 to 1800/1 when the ratio was measured under steady state conditions. The change in the ratio could be due either to a change in the denominator or a change in the numerator of the ratio. The results of the recurrent multiscaling experiments (to be reported later) showed that the delayed light emission term (the denominator) was the term responsible for the change in the fluorescence/delayed light ratio.

Recurrent Multiscaling

The experimental procedure for the recurrent multiscaling experiments was to make four 1-minute duration recordings of the first five milliseconds of delayed light emission during the first eleven minutes of the light induction period. It was found that the recording of the delayed light emission of the first minute of the induction period produced a decay curve of amplitude higher than any of the other three recordings. Furthermore, the last three curves were always found to be virtually superimposible. This showed that the loss of amplitude of the delayed light emission curve was completed within the first two minutes of exposure of the algae to the modulated stimulus light, i.e., the loss of amplitude of the delayed light emission curve was complete before the recording of the second curve during

the third minute of illumination. Since the last three curves did not differ appreciably, the last recording was compared to the first recording in order to compare the delayed light emission of the first minute of the induction period to the delayed light emission of the eleventh minute of the induction period. Since no adjustments were made on the instrumentation during the eleven minute induction period, and since the same sample was used for each eleven minute induction period, the data from the first minute of the induction period could be compared directly to the data of the eleventh minute. Therefore, the data from the two recordings were normalized by the same factor in order to fit a three-cycle logarithmic ordinate scale. Display of the data of the two recordings of each set of experiments allowed direct comparison of the kinetics of the two experiments by comparison of the two data curves.

Figure 16 illustrates the results of the first repetitive multiscaling experiments for the wildtype algae under induction conditions of illumination with an instantaneous stimulus light of 0.11 mW/cm^2 at the algal sample. The two curves of Figure 16 have virtually the same curvature and slopes when plotted together on the logarithmic ordinate plot. The identical curvature and slope of the two curves implies that the two curves represent identical kinetics for the delayed light emission during the first and eleventh minute of the induction period. Since the eleventh minute recording

produced data which plotted lower on the logarithmic plot than the first minute recording data, one can conclude that the two curves show similar kinetics of delayed light emission but differ in the absolute magnitude of the delayed light emission.

In the set of experiments with the 2.25 mW/cm^2 stimulus light, the delayed light emission changed in amplitude between the first and fourth recording by such a small amount that the plot of the data of the recordings, shown in Figure 17, shows the two curves overlapping.

Figure 18 shows the results of the experiment set utilizing 22.5 mW/cm^2 laser light stimulus. One can see that the majority of the change in amplitude of the delayed light emission curve occurred between the first and eleventh minute of the light induction period. In this case, however, one can see that the two curves have the same slope in the left third of the figure, but they then diverge slightly in the rest of the plot.

The most intense stimulus light, 59 mW/cm^2, was used in the experiments described by the curves in Figure 19. The two curves have slopes and divergence identical to the two curves of the previous experiment which utilized 22.5 mW/cm^2 excitation laser light. Thus, the delayed light emission induction seems to have been saturated at the 22 mW/cm^2 stimulus light level.

Figure 16. Comparison of the first minute (upper curve) and the eleventh minute (lower curve) of wildtype algal delayed light emission during the induction period of an experiment utilizing 0.11 mW/cm^2 instantaneous intensity of stimulus laser light.

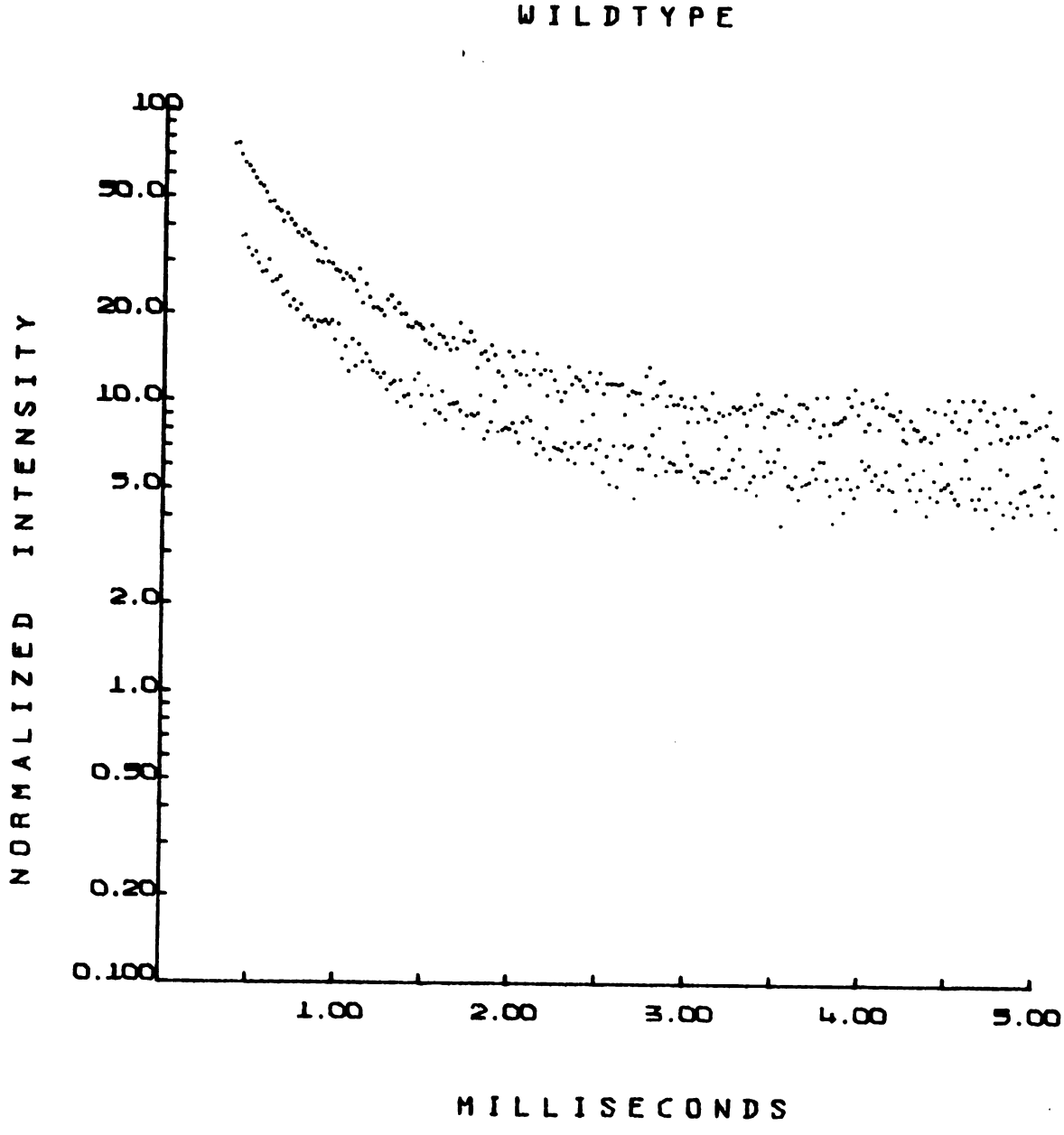
WILDTYPE
NORMALIZED INTENSITY
100
50.0
20.0
10.0
5.0
2.0
1.0
0.50
0.20
0.100
1.00
2.00
3.00
4.00
5.00
MILLISECONDS

Figure 17. Comparison of the first minute (upper curve) and the eleventh minute (lower curve) of wildtype algal delayed light emission during the induction period of an experiment utilizing 2.25 mW/cm^2 instantaneous intensity of stimulus laser light. The two curves are so close on the plot that they appear to be a single wide curve.

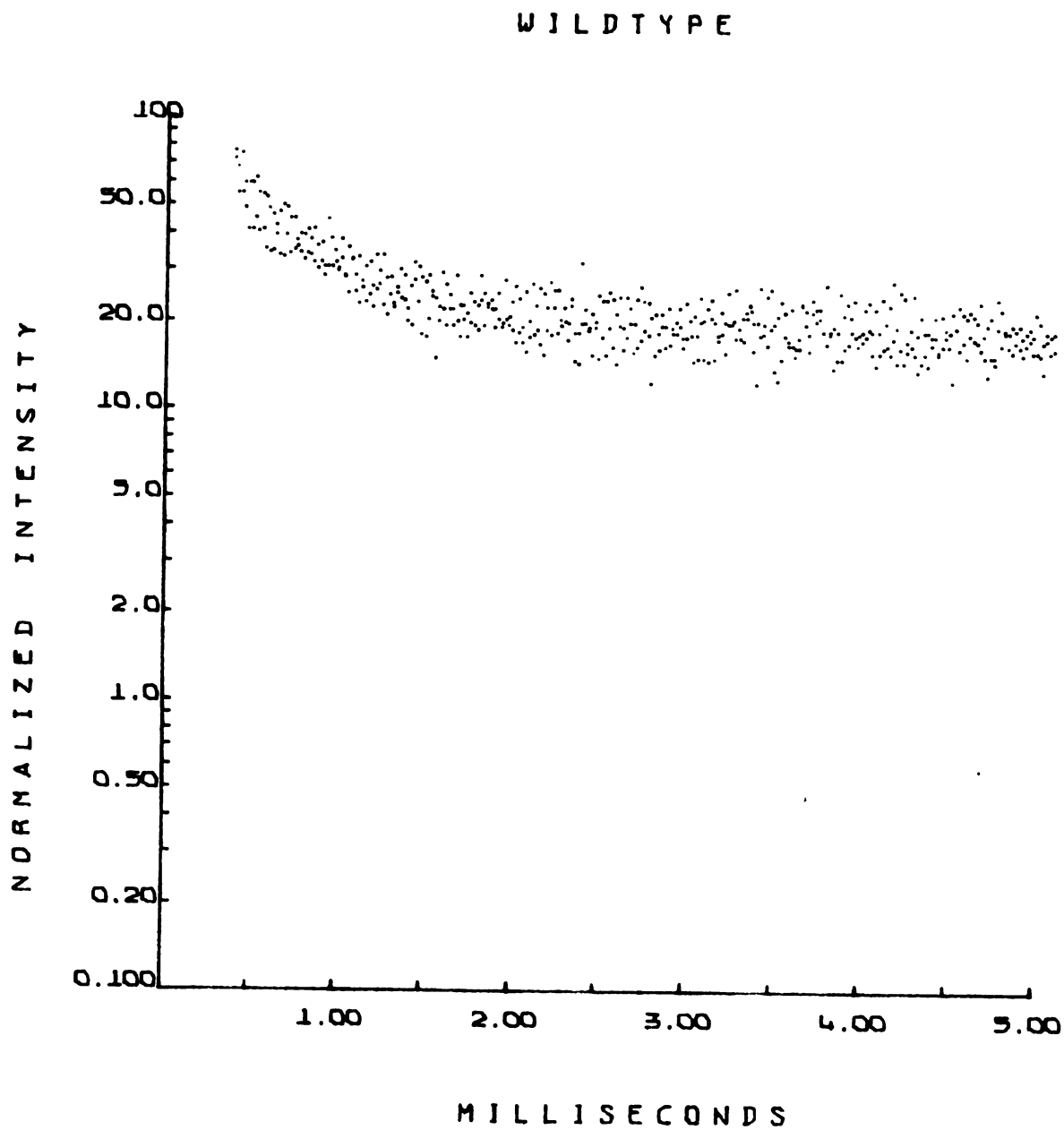
WILDTYPE
NORMALIZED INTENSITY
100
50.0
20.0
10.0
5.0
2.0
1.0
0.50
0.20
0.100
1.00
2.00
3.00
4.00
5.00
MILLISECONDS

Figure 18. Comparison of the first minute (upper curve) and the eleventh minute (lower curve) of wildtype algal delayed light emission during the induction period of an experiment utilizing 22.5 mW/cm^2 instantaneous intensity of stimulus laser light.

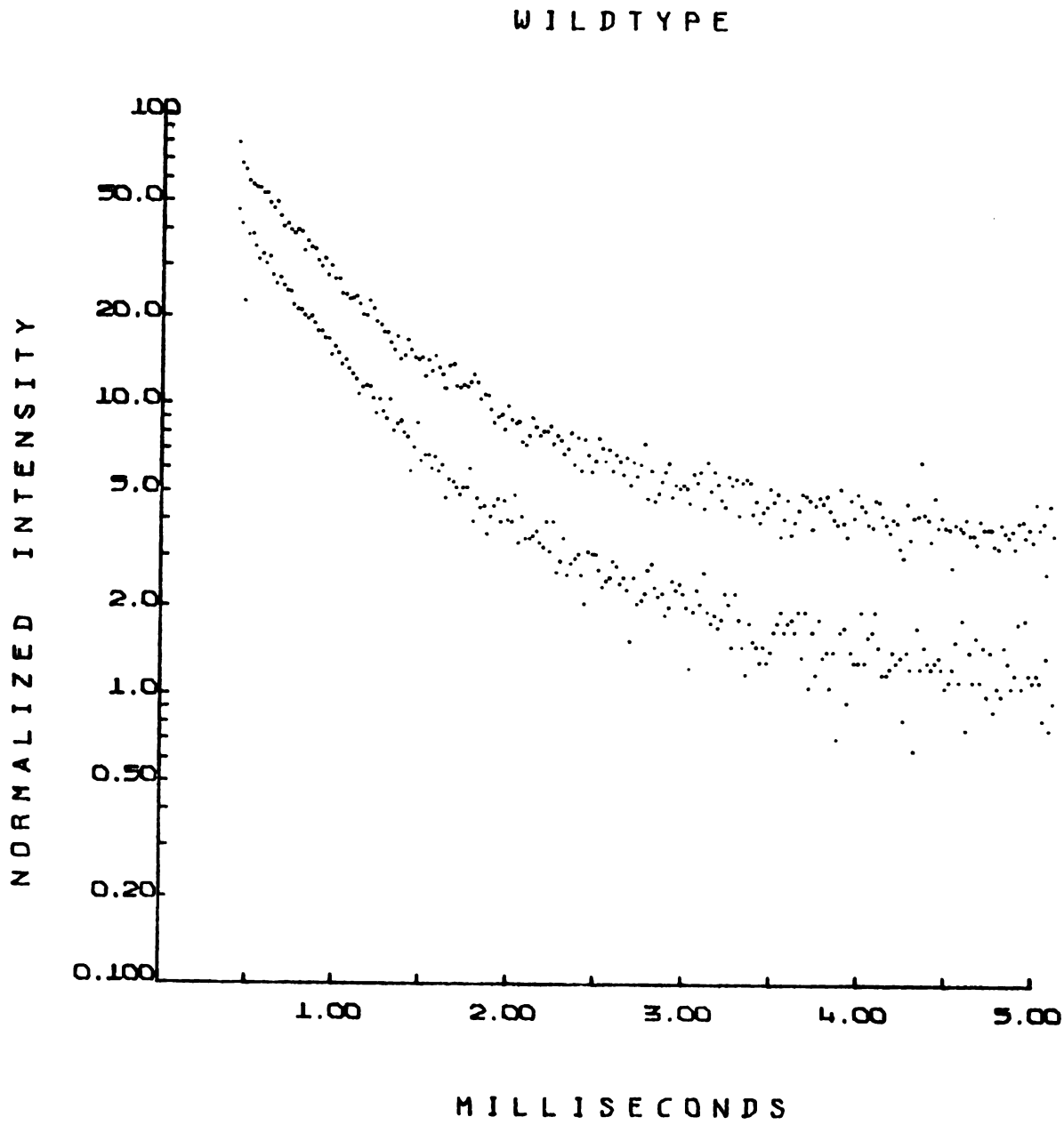
WILDTYPE
NORMALIZED INTENSITY
100
50.0
20.0
10.0
5.0
2.0
1.0
0.50
0.20
0.100
1.00
2.00
3.00
4.00
5.00
MILLISECONDS

Figure 19. Comparison of the first minute (upper curve) and the eleventh minute (lower curve) of wildtype algal delayed light emission during the induction period of an experiment utilizing 59 mW/cm^2 instantaneous intensity of stimulus laser light.

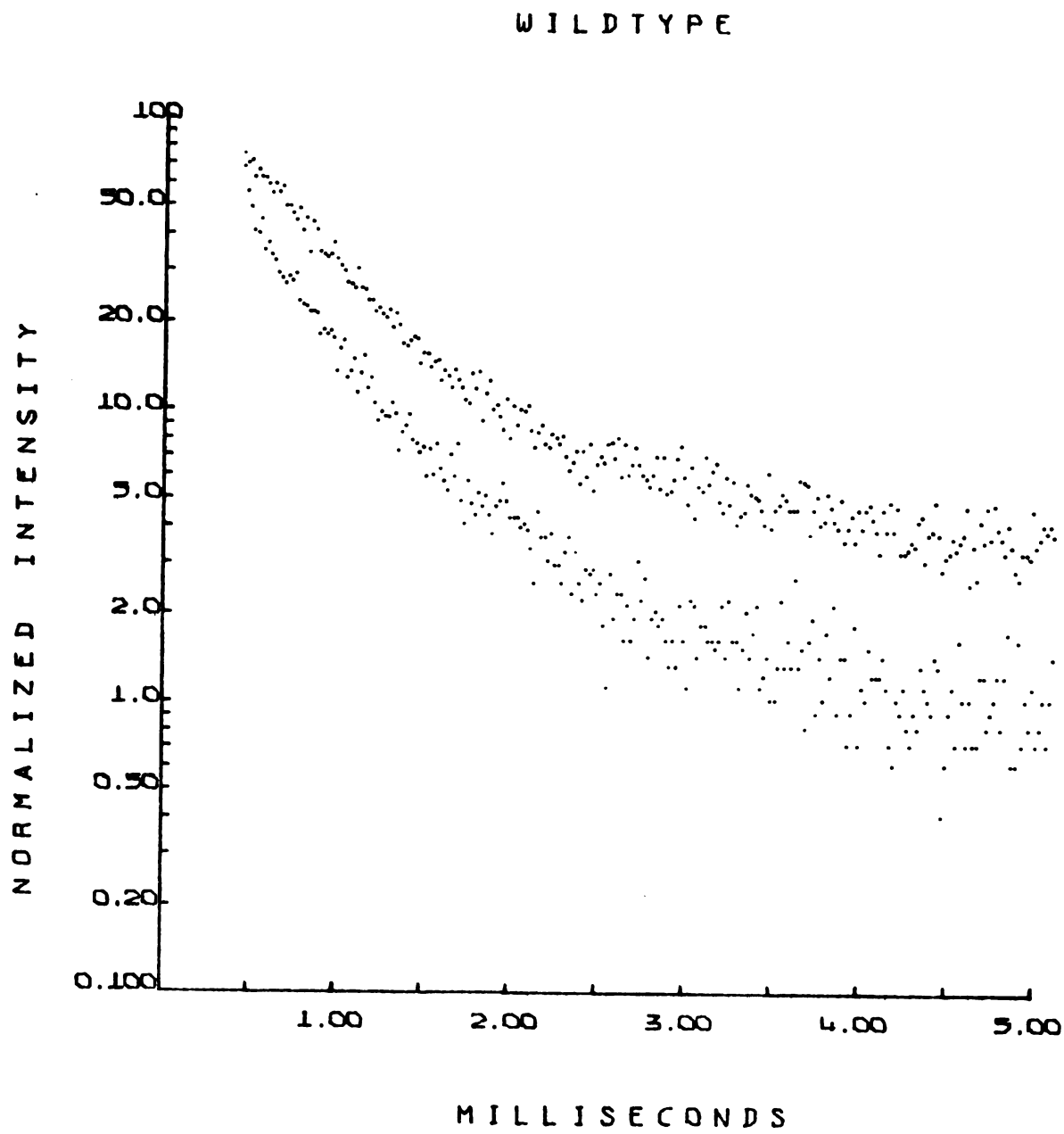
WILDTYPE
NORMALIZED INTENSITY
100
50.0
20.0
10.0
5.0
2.0
1.0
0.50
0.20
0.100
1.00
2.00
3.00
4.00
5.00
MILLISECONDS

Figure 20. Comparison of the first minute (upper curve) and the eleventh minute (lower curve) of mutant 8 algal delayed light emission during the induction period of an experiment utilizing 22.5 mW/cm^2 instantaneous intensity of stimulus laser light.

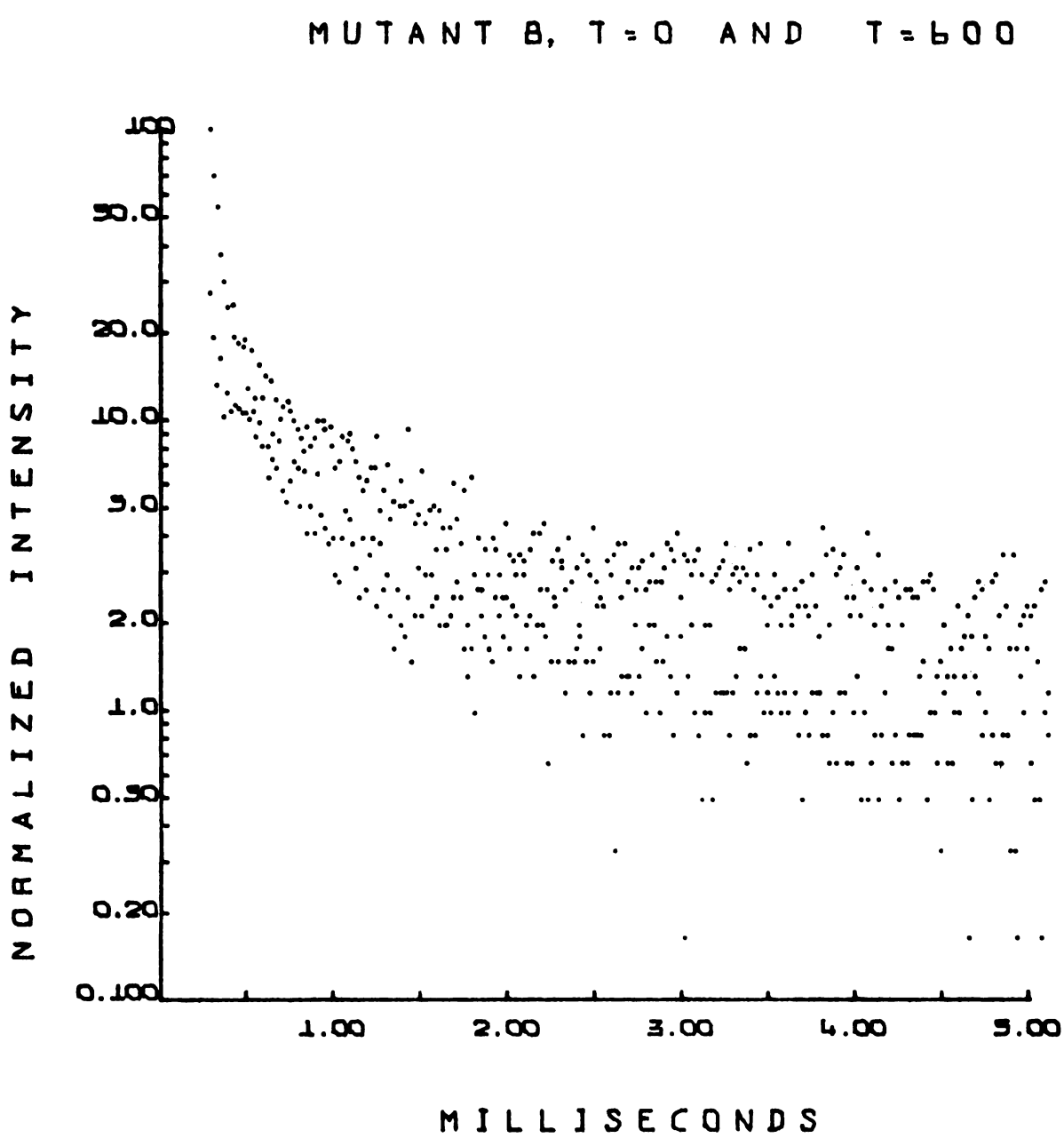
MUTANT B, T = 0 AND T = 600
NORMALIZED INTENSITY
1.00
2.00
3.00
4.00
5.00
MILLISECONDS

The last set of experiments report the data from the experiments utilizing the mutant 8 algae. Figure 20 shows the curve of the delayed light emission from mutant 8 algae during stimulus with 22.5 mW/cm^2 laser light. Two items of interest can be seen in this plot. First, the rather small spacing between the two curves indicates that there was only a small decrease in amplitude of the eleventh minute recording as compared to the first minute recording. Second, there seems to be a rather large amplitude component in the first minute recording in the area of the first 150 microseconds of the delayed light emission curve, i.e., in the first seven or eight dots of the curve. But in the eleventh minute curve, i.e., of the experiment initiated at the 600 second mark in the light induction period, the 150 microsecond component has almost disappeared. The amplitude of the initial 150 microseconds of the delayed light emission curve decayed by a factor of four in a period of 600 seconds. The kinetics of this 150 microsecond component of the mutant 8 algae are reported in detail in the next section of the results chapter.

Single Sweep Multiscaling

The purpose of the single sweep multiscaling experiments was to utilize an electronic gate signal in order to segregate a particular part of the delayed light emission and then to record the discriminator pulses representing the

segregated time interval of the delayed light emission over the duration of the 820-second light induction period.

The first data presented is that of an experiment in which the gate signal for the discriminator was positioned in the time period during which the dark-adapted wildtype algae were still being illuminated by the modulated stimulus laser light. From Figure 21, one can see that the prompt fluorescence from the wildtype algae reached a maximum intensity in about 60 seconds, and remained rather constant at this level of intensity for the remaining portion of the 820-second light induction period.

The second set of data show the analogous experiment utilizing the dark-adapted mutant 8 algae. Figure 22 shows that the transition of the prompt fluorescence to its maximum was not as pronounced as that of the wildtype, even though both algal samples were exposed to the same 11.7 mW/cm^2 instantaneous intensity of modulated laser light.

Figure 23 shows the normalized data from an experiment in which the electronic gating signal was adjusted to occur immediately following stimulus light extinction. Thus, the discriminator pulses which occurred in the 60-microsecond wide gate signal were those of delayed light emission. The plot shows that the delayed light emission from the dark-adapted wildtype algae decreased during the first twenty to thirty seconds of exposure of the dark-adapted cells to the

modulated laser light. But the intensity of the delayed light emission recovered within two hundred seconds to a level of intensity greater than the intensity of the first seconds of the light induction period.

Figure 24 shows the results of the analogous experiment in which the gating signal allowed only the first 60 microsecond portion of the delayed light emission curve to be recorded during the 820-second induction period. One can see that the intensity of the delayed light emission began to fall immediately after the stimulus light was applied, and there was no recovery in intensity as there was in the case of the wildtype algae. The curve shown in Figure 24 had not reached a plateau even at the end of the 820-second induction period.

In order to determine whether the intensity of the delayed light emission could show recovery toward the original amplitude during periods of darkness, several experiments were run in which the modulated stimulus light was blocked from the algal sample for periods of 30 seconds, 60 seconds, 90 seconds, and 120 seconds. Figures 25 to 27 show the results of these experiments in which the instantaneous intensity of stimulus laser light at the sample was 4.5, 30, and 45 mW/cm^2 respectively. In these experiments, the increase in stimulus light intensity was exactly compensated for by the progressive closure of the iris in front

of the photomultiplier tube so that the total number of counts per second from the tube was the same for all three experiments. This procedure allowed the light emission detection to operate under similar conditions in each of the experiments, and the data from each experiment was of the same order of magnitude. Note that, after the periods of darkness, the intensity of delayed light emission was temporarily restored toward the level of intensity of the first seconds of the experiment. It should be noted also that the recovery of intensity of delayed light emission was progressively greater for the periods of darkness up to 90 seconds. But the 120-second period of darkness did not cause a greater restoration of intensity of delayed light emission than the 90 second period.

Figure 21. Gated interval of wildtype algal fluorescence during the induction period.

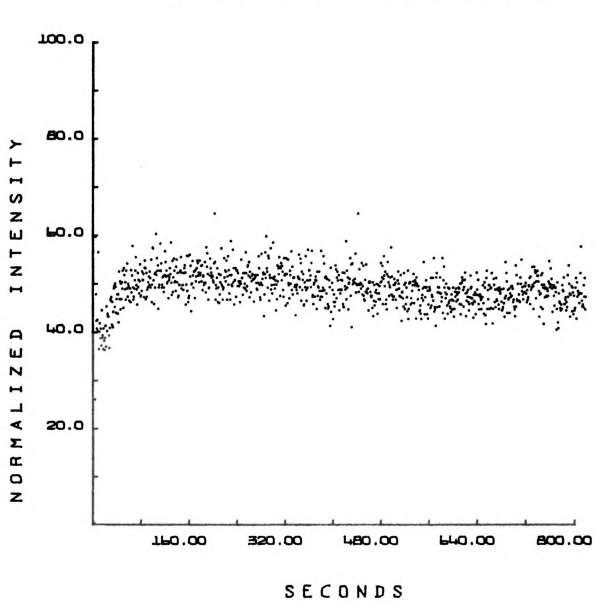
WILDTYPE FLUORESCENCE
NORMALIZED INTENSITY
100.0
80.0
60.0
40.0
20.0
160.00
320.00
480.00
640.00
800.00
SECONDS

Figure 22. Gated interval of mutant 8 algal fluorescence during the induction period.

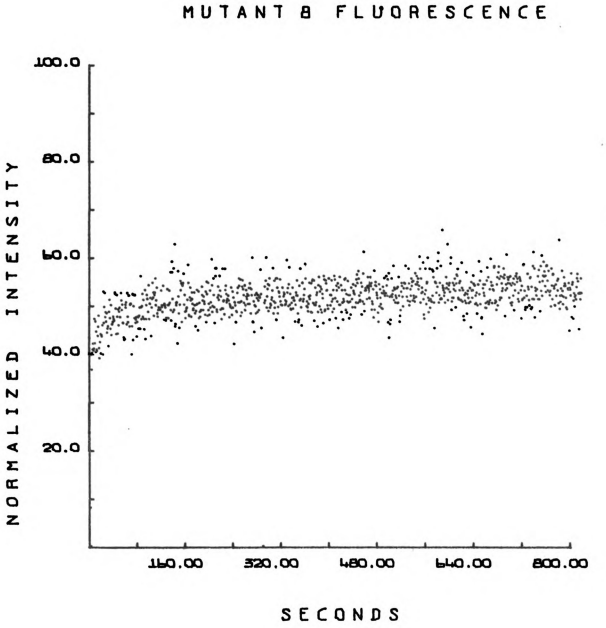
MUTANT B FLUORESCENCE
NORMALIZED INTENSITY
100.0
80.0
60.0
40.0
20.0
160.00
320.00
480.00
640.00
800.00
SECONDS

Figure 23. Gated interval of wildtype algal delayed light emission during the induction period.

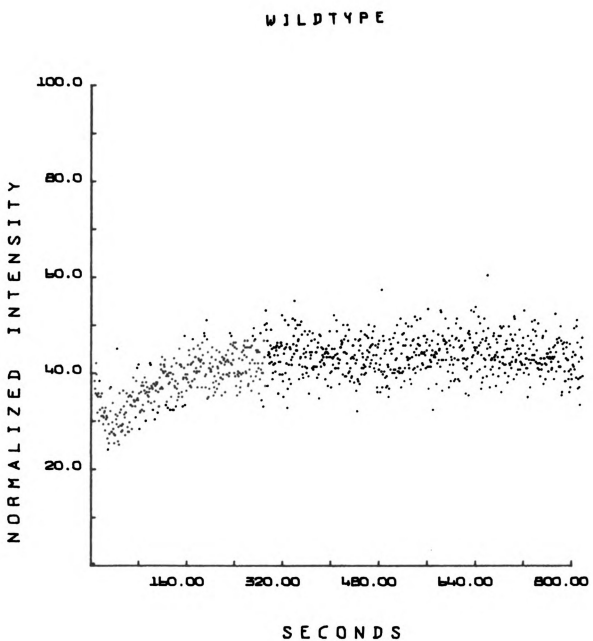
WILDTYPE
100.0
80.0
60.0
40.0
20.0
NORMALIZED INTENSITY
160.00
320.00
480.00
640.00
800.00
SECONDS

Figure 24. Gated interval of mutant 8 algal delayed light emission during the induction period.

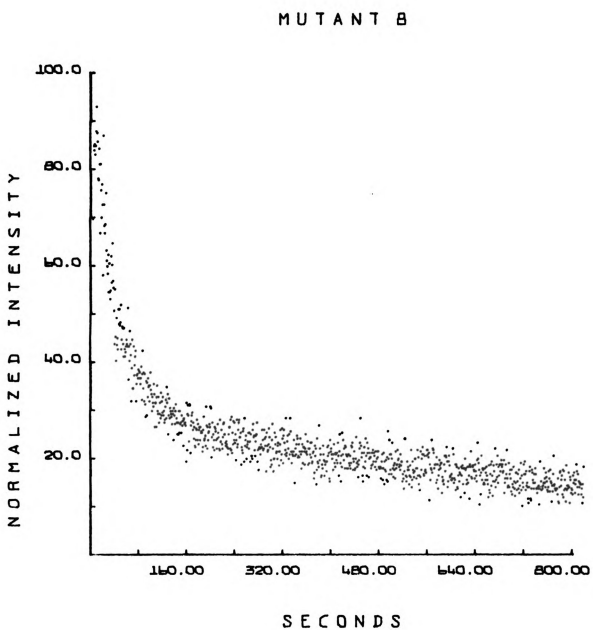
MUTANT 8
NORMALIZED INTENSITY
100.0
80.0
60.0
40.0
160.00
320.00
480.00
640.00
800.00
SECONDS

Figure 25. The decay and recovery of a gated interval of delayed light emission from mutant 8 algae during the induction period of an experiment utilizing 4.5 mW/cm^2 instantaneous intensity of stimulus laser light. The gaps in the curve occurred when the excitation laser beam was blocked for periods of 30, 60, 90, and 120 seconds.

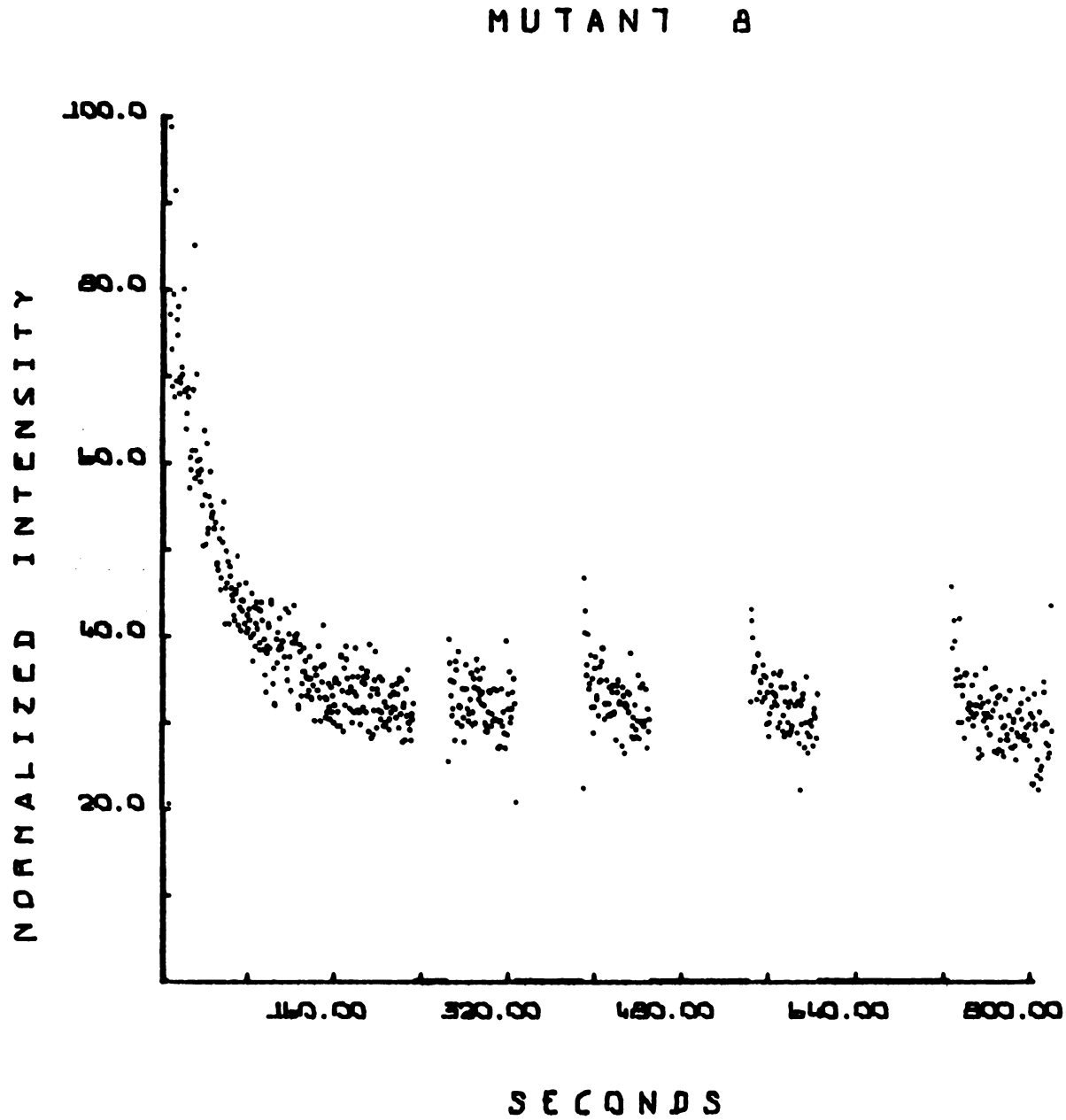
MUTANT B
NORMALIZED INTENSITY
100.0
80.0
60.0
40.0
20.0
160.00
320.00
480.00
640.00
800.00
SECONDS

Figure 26. The decay and recovery of a gated interval of delayed light emission from mutant 8 algae during the induction period of an experiment utilizing 30 mW/cm^2 instantaneous intensity of stimulus light.

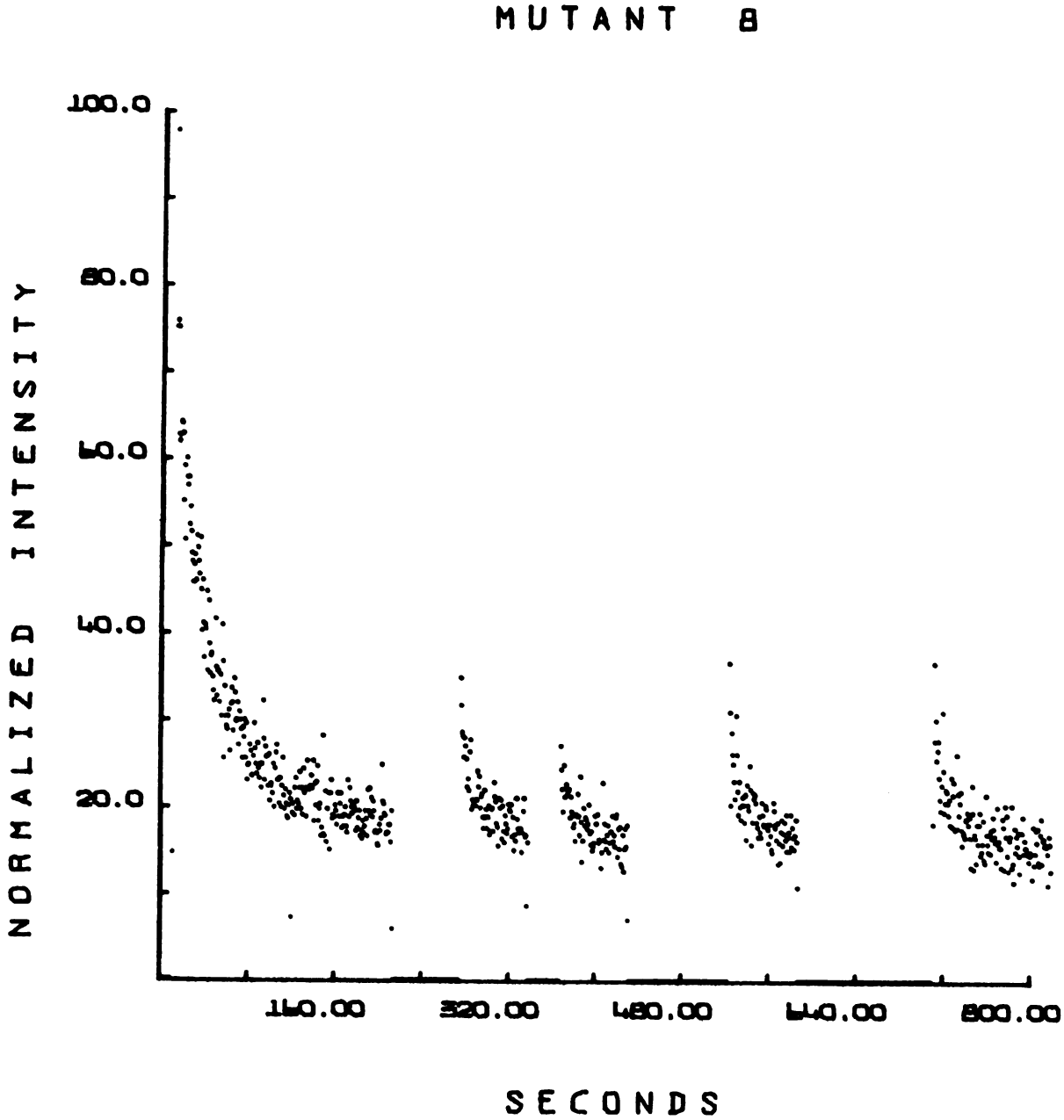
MUTANT 8
NORMALIZED INTENSITY
100.0
80.0
60.0
40.0
20.0
160.00
320.00
480.00
640.00
800.00
SECONDS

Figure 27. The decay and recovery of a gated interval of delayed light emission from mutant 8 algae during the induction period of an experiment utilizing 45 mW/cm^2 instantaneous intensity of stimulus light.

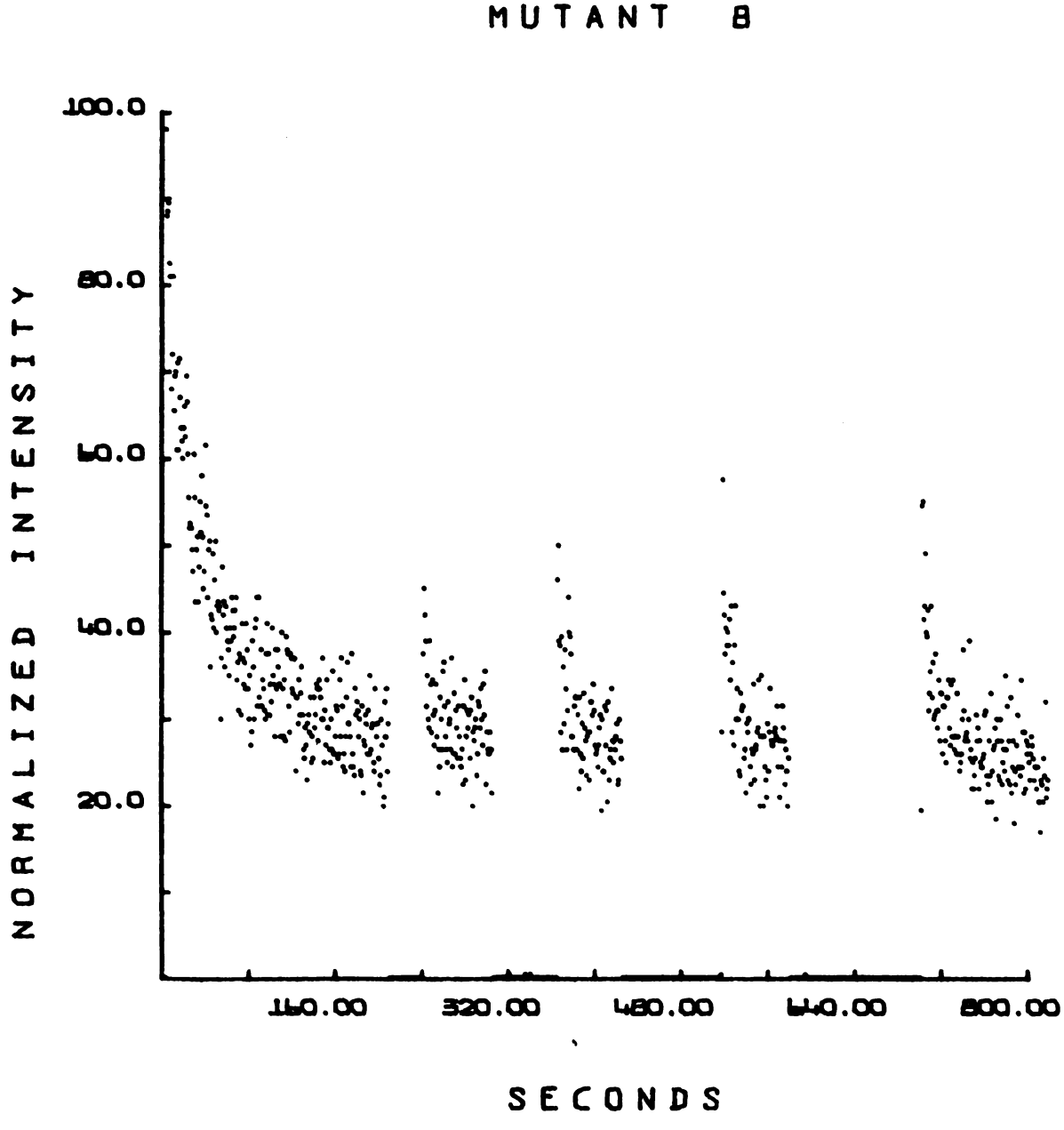
MUTANT B
100.0
80.0
60.0
40.0
20.0
NORMALIZED INTENSITY
160.00
320.00
480.00
640.00
800.00
SECONDS

DISCUSSION

The following discussion will cover the experimental results in the order the results were presented, beginning with the pulse-height analysis experiments, and ending with the single sweep multiscaling experiments. The entire course of the discussion will be concerned with how the experimental results could be intrepreted in relation to the basic premise of this thesis: that the intensity of delayed light emission reflected the rate of electron flow through photosystem II. The basic extensions of this hypothesis were discussed in the introduction chapter and the reasoning of the various experiments was discussed in the introduction chapter in detail.

The pulse-height analysis experiments' kinetics of prompt fluorescence and of delayed light emission close to the instant of stimulus light extinction were such that one could conclude that the delayed light emission was a process that occurred during illumination of the algal sample, but that the emission could not be detected until the more intense prompt fluorescence was eliminated when the stimulus light was extinguished. The demonstration TAC experiments allowed

comparison of the level of delayed light to the level of photon counting system noise and the experiments also showed that the ratio of prompt fluorescence intensity to the intensity of the first microsecond of delayed light emission was between 200:1 to 100:1.

The results of pulse-height analysis experiments were combined with the results of photodiode-sampling scope experiments in order to more closely calculate the ratio of prompt fluorescence to the first microsecond of delayed light intensity. The calculated ratios supported the hypothesis that the wildtype algae should maintain a rather constant ratio during steady state conditions of stimulus illumination, while the mutant 8 algae were not expected to show a constant ratio. The experiments were repeated with dark-adapted algae in the flow conditions, and the results were again what were expected: the wildtype algae showed about the same ratio of prompt fluorescence to delayed light emission as in steady state conditions of illumination, whereas the mutant 8 ratio was different from the ratios obtained under steady state conditions of illumination.

According to the hypothesis, the first seconds of illumination of dark-adapted algae would be expected to produce the highest intensity of delayed light emission due to the highest possible rate of electron flow through photosystem II. The high flow of electrons should be detected as

the highest intensity of delayed light emission, if the hypothesis is correct. The recurrent multiscaling experiments showed that the kinetics of delayed light emission did not change during the first eleven minutes of induction, but that the absolute magnitude of the delayed light did decrease. Moreover, the intensity of delayed light emission decreased during the first seconds of the induction period in such a manner that the recordings taken during the third, sixth, and eleventh minutes of the light induction period were virtually identical. The similarity of the kinetics of the recurrent multiscaling recordings of each experimental set prompted the conclusion that there was only one mechanism operative in the production of delayed light emission throughout the induction period.

The single sweep multiscaling experiments showed that the first 60 microseconds of the delayed light emission did not correspond in its kinetics during the induction period to the prompt fluorescence of the wildtype algae under the same intensity of illumination. This argued against the idea that the intensity of delayed light emission strictly depended upon the condition of the photosystem II traps. Instead, the results gave support to the hypothesis that the delayed light intensity was an indication of the rate of electron flow through photosystem II. Compare the prompt fluorescence curve and the delayed light emission curve

for the wildtype algae during the induction period (Figures 21 and 23). The two curves do not show any direct or inverse relationship, even though the data was from algal samples of the same batch of dark-adapted algae and even though the stimulus light intensity was identical in the two experiments. An inspection of the mutant 8 curves, however, shows the situation obtained when photosystem I was inactive. In this case, the initial decline in delayed light intensity continued without recovery. Eventually the delayed light intensity reached a rather stable baseline level. In contrasting the results of the wildtype with those of the mutant 8 algae, one would be tempted to postulate that the induction period recovery seen in the wildtype delayed light emission curve was due to the effect of photosystem I coming into play and establishing a path of reoxidization for the somewhat reduced electron transport chain components.

The last set of experiments showed that the mutant 8 delayed light emission could recover somewhat during periods of darkness. This evidence, together with the rapid rate of decay in the delayed light intensity during the first two minutes of the induction period, gave support to the hypothesis that the periods of darkness allowed the pool of the electron acceptor compound, A, to somewhat reoxidize. The reoxidization of a small percentage of the total pool of the electron acceptor compound resulted in a temporary

higher rate of electron flow during the first few seconds after illumination was restored. The higher rate of electron flow resulted in a more intense delayed light emission.

Amez et al. (63) have proposed that the electron acceptor compound A is identical to plastoquinone and that plastoquinone is the only large pool in the electron transport chain between the two photosystems. Plastoquinone is known to be located at the start of the electron transport chain, close to Q. The experiments of the last section of the thesis showed that the gated portion of the mutant 8 delayed light emission eventually reached a plateau level. This suggests that the pool of A is not homogeneous, in agreement with the finding of Forbush and Kok (32). If the rapidly decaying component of pool A does form a separate component of the pool, the 80 microsecond TAC flow experiments gave an estimate of the decay constant of the rapidly decaying component of the A pool. The decay constant of the other component of the A pool could be determined from steady state TAC experiments with mutant 8 algae, since the preillumination should have exhausted the rapidly decaying component from the pool A.

That delayed light emission is a reflection of the rate of electron transport through photosystem II is a hypothesis that is not without precedent in its correlation of an observable parameter of photosynthesis with electron

flow. The rate of oxygen evolution, the intensity of prompt fluorescence, the intensity of delayed light emission, and the rate of photophosphorylation are functions of the rate of electron flow from photosystem II to photosystem I. Arnon (64) showed that, in isolated chloroplasts, the oxygen evolution rate was highest under conditions which were optimal for the simultaneous formation of ATP, or under conditions where electron transport was uncoupled from phosphorylation. Mayne (65) has explored the effect of photosynthesis inhibitor compounds and has found that electron acceptors, such as ferricyanide, increased delayed light emission, while inhibitors of electron transport, such as DCMU, and uncouplers of photophosphorylation decreased delayed light emission intensity.

The experimental results reported in this thesis depended upon the development of the photon-counting instrumentation. This thesis work is the first report of the nanosecond and microsecond components of delayed light emission, and the success in the measurement of this emission was due to the photon-counting instrumentation which allowed the direct measurement of the delayed light emission without any assumptions as to the emission being exponential. The photon-counting instrumentation also enabled the recording of specific components of the delayed light emission, from one microsecond to several milliseconds,

or of specific components of the prompt fluorescence. One must appreciate that the large dynamic range of the photon-counting apparatus allowed the measurement of either prompt fluorescence or delayed fluorescence, from the same sample, with equal ease. The application of the photon-counting technique should stimulate research into the delayed light emission process and its mechanism.

In summary, past researches have shown that delayed light emission is associated with the first steps of photosynthesis, and the study of delayed light emission seems to be one of the few ways of studying the early steps of photosynthesis. In past years (66-68), data from the delayed light emission experiments have helped shape the theories concerning the operation of the photosynthetic mechanism.

LIST OF REFERENCES

LIST OF REFERENCES

1. G. G. Stokes, Proc. Roy. Soc. (London), 13, 144 (1964).
2. B. L. Strehler and W. Arnold, J. Gen. Physiol., 34, 809 (1951).
3. R. K. Clayton, J. Gen. Physiol., 48, 633 (1965).
4. W. Arnold and J. B. Davidson, J. Gen. Physiol., 37, 677 (1954).
5. W. F. Bertsch, J. R. Azzi and J. B. Davidson, Biochim. Biophys. Acta, 143, 129 (1967).
6. P. B. Sweetser, C. W. Todd and R. T. Hersh, Biochim. Biophys. Acta, 51, 509 (1961).
7. W. E. Arthur and B. L. Strehler, Arch. Biochem. Biophys., 70, 507 (1957).
8. W. F. Bertsch and J. R. Azzi, Biochim. Biophys. Acta., 94, 15 (1965).
9. G. N. Lewis, D. Lipsin and T. T. Magel, J. Am. Chem. Soc., 63, 3005 (1941).
10. C. A. Parker, Proc. Roy. Soc. (London), A276, 125 (1963).
11. C. A. Parker and C. G. Hatchard, J. Phys. Chem., 66, 2506 (1962).
12. W. Arnold and J. R. Azzi, Proc. Natl. Acad. Sci., 61, 29 (1968).
13. W. Arnold, Photochem. Photobiol., 14, 233 (1971).
14. W. Arnold and H. Sherwood, J. Phys. Chem., 63, 2 (1959).
15. W. Arnold, J. Phys. Chem., 69, 788 (1965).

16. B. L. Strehler, Arch. Biochem. Biophys., 34, 239 (1951).

17. J. C. Goedheer, Biochim. Biophys. Acta, 64, 294 (1962).

18. B. C. Mayne and R. K. Clayton, Proc. Natl. Acad. Sci., 55, 494 (1966).

19. G. P. Kraan, J. Amesz, B. R. Velthuys and R. G. Steemers, Biochim. Biophys. Acta, 223, 129 (1970).

20. J. Barber, Biochim. Biophys. Acta, 275, 105 (1972).

21. G. W. Robinson, Proc. Natl. Acad. Sci., 49, 521 (1963).

22. G. W. Robinson, Ann. Rev. Phys. Chem., 15, 311 (1964).

23. G. W. Robinson, Biophys. J., 9, 521 (1969).

24. W. T. Stacy, T. Mar, C. E. Swenberg and Govindjee, Photochem. Photobiol., 14, 197 (1971).

25. L. W. Jones, Proc. Natl. Acad. Sci., 58, 75 (1967).

26. R. H. Ruby, Photochem. Photobiol., 8, 299 (1968).

27. R. H. Ruby, Photochem. Photobiol., 13, 97 (1971).

28. R. Hill and D. Bendall, Nature, 186, 136 (1960).

29. J. Lavorel and R. P. Levine, Plant Physiol., 43, 1049 (1968).

30. P. Joliot, Biochim. Biophys. Acta, 102, 116 (1965).

31. D. C. Fork, Plant Physiol., 38, 323 (1963).

32. B. Forbush and B. Kok, Biochim. Biophys. Acta, 162, 243 (1968).

33. L. N. M. Duysens, in "Photosynthetic Mechanisms of Green Plants", Natl.Acad. Sci. Natl. Res. Council Publ. 1145, Washington, D. C., (1963).

34. N. I. Bishop, Record Chem. Progr. (Kresge-Hooker Sci. Lib.), 25, 181 (1964).

35. R. P. Levine, Ann. Rev. Plant Physiol., 20, 523 (1969).

36. N. I. Bishop and J. Wong, Biochim. Biophys. Acta, 234, 433 (1971).

37. R. Powls, J. Wong and N. I. Bishop, Biochim. Biophys. Acta, 180, 490 (1969).

38. W. Arnold and J. B. Davidson, in "Photosynthetic Mechanisms of Green Plants", Natl. Acad. Sci. Natl. Res. Council Publ. 1145, Washington, D. C. (1963).

39. A. Müller and R. Lumry, Proc. Natl. Acad. Sci., 54, 1479 (1965).

40. W. Arnold, Biophys. J., 12, 793 (1972).

41. P. Joliot, Biochim. Biophys. Acta, 102, 135 (1965).

42. R. K. Clayton, Biophys. J., 9, 60 (1969).

43. R. R. Alfano and N. Ockman, J. Opt. Soc. Amer., 58, 90 (1968).

44. T. Tao, Biopolymers, 8, 609 (1969).

45. X. J. Yguerabide, H. F. Epstein and L. Stryer, J. Mol. Biol., 51, 573 (1970).

46. G. K. Grau, Appl. Opt., 4, 755 (1965).

47. D. L. Fired, Appl. Opt., 4, 79 (1965).

48. G. A. Morton, Appl. Opt., 7, 1 (1968).

49. J. A. Tapp, H. W. Schrotter, H. Hacker and J. Brandmuller, Rev. Sci. Instr., 40, 1164 (1969).

50. M. R. Zatzick, Res. Devel., 21, 16 (1970).

51. M. R. Zatzick, Appl. Note 71021, SSR Instr. Co., Santa Monica, Calif. (1971).

52. M. R. Zatzick, Elect. Opt. Syst. Design, 4, 20 (1972).

53. ORTEC Appl. Note AN35, ORTEC, Inc., Oak Rodge, Tenn. (1971).

54. M. L. Franklin, G. Horlick and H. V. Malmstadt, Anal. Chem., 41, 2 (1969).

55. E. H. Eberhardt, Appl. Opt., 6, 251 (1967).

56. J. P. Rodman and H. J. Smith, Appl. Opt., 2, 181 (1963).

57. F. T. Arechi, E. Gatti and A. Sona, Rev. Sci. Instr., 37, 942 (1966).

58. J. K. Nakamura and S. E. Schwarz, Appl. Opt., 7, 1073 (1968).

59. F. DeMartini and K. P. Wacks, Rev. Sci. Instr., 38, 866 (1967).

60. N. Klein and T. J. Rock, Rev. Sci. Instr., 41, 1671 (1970).

61. L. H. Pratt and N. I. Bishop, Biochim. Biophys. Acta, 153, 664 (1968).

62. H. Kaltwasser, T. S. Stuart and H. Graffron, Planta, 89, 309 (1969).

63. J. Amesz, J. W. Visser, G. J. van den Engh and M. P. Dirks, Biochim. Biophys. Acta, 256, 370 (1972).

64. D. I. Arnon, F. R. Whatley and M. B. Allen, Science, 127, 1026 (1958).

65. B. C. Mayne, Photochem. Photobiol., 6, 189 (1967).

66. R. K. Clayton, Science, 149, 1346 (1965).

67. W. F. Bertsch, Proc. Natl. Acad. Sci., 48, 2000 (1962).

68. R. K. Clayton, Photophysiol., 1, 155 (1964).